Nanoscale

Accepted Manuscript

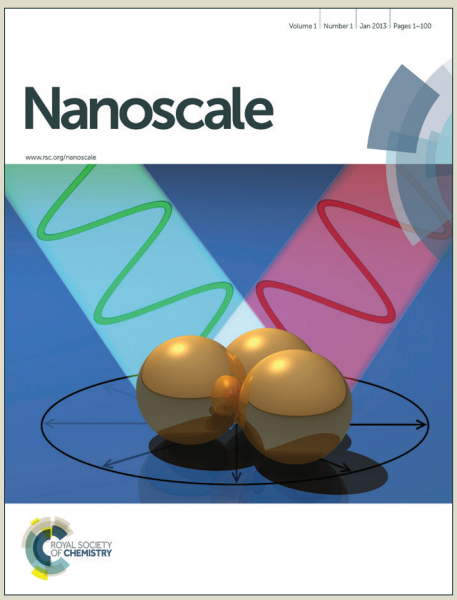

ROYAL SOCIETY OF CHEMISTRY

www.rsc.org/nanoscale

Smart multifunctional drug delivery towards anticancer therapy harmonized in mesoporous nanoparticles

Seonmi Baek[1,#], Rajendra K. Singh[2,3,#], Dipesh Khanal[1], Kapil D. Patel[2,3], Eun-Jung Lee[2,3], Kam Leong[2,4], Wojciech Chrzanowski[1,2,*], Hae-Won Kim[2,3,5,*]

[1] Faculty of Pharmacy, The University of Sydney, NSW 2006, Australia

[2]Department of Nanobiomedical Science & BK21 Plus NBM Global Research Center for Regenerative Medicine, Dankook University, Cheonan 330-715, Republic of Korea

[3]Institute of Tissue Regenerative Engineering (ITREN), Dankook University, Cheonan 330-715, Republic of Korea

[4] Department of Biomaterials Science, College of Dentistry, Dankook University, Cheonan, 330-715, Republic of Korea

[5] Department of Biomedical Engineering, Columbia University, New York, NY 10027, USA

[#] Authors (Baek S and Singh RK) contributed equally to this work

[*]Corresponding authors: Chrzanowski W (wojciech.chrzanowski@sydney.edu.au) and Kim HW (kimhw@dku.edu)

Abstract

Nanomedicine seeks to apply nanoscale materials for the therapeutic and diagnostic purposes of diseased and damaged tissues. Recent advances in nanotechnology have made a major contribution to the development of multifunctional nanomaterials, which represents a paradigm shift from single purpose to multipurpose materials. Multifunctional nanomaterials have been proposed to enable simultaneous target imaging and on-demand delivery therapeutic agents only to the specific site [1]. Most advanced systems are also responsive to internal or external stimuli. This approach is particularly important for highly potent drugs (e.g. chemotherapeutics), which should be delivered in discreet manner, and interact with cells / tissues locally only. Both advances in imaging and precisely controlled and localized delivery are critically important in cancer treatment, and the use of such systems – theranostics – holds great promise to significantly reduce severe side effects of the dreary treatment whilst boosting the treatment effectiveness. Among others, mesoporous silica nanoparticles (MSNPs) are considered one of the most promising nanomaterials for drug delivery. Due to their unique intrinsic features, including tunable porosity and size, large surface area, structural diversity, easily modifiable chemistry and suitability for functionalization, and biocompatibility, MSNPs have been extensively utilized as multifunctional nanocarrier systems. The combination or hybridization with biomolecules, drugs, and other nanoparticles potentiated the ability of MSNPs towards multifunctionality, and even smart actions stimulated by specified signals, including pH, optical signal, redox reaction, electricity and magnetism. This paper provides the comprehensive review of state-of-art of multifunctional, smart drug delivery systems centered on advanced MSNPs, with special emphasis on cancer related applications.

Keywords

Theranostics; Multifunctional materials; Mesoporous silica nanoparticles; Stimuli responsiveness; Cancer treatment; smart materials; controlled drug delivery; Biocompatible materials

1. Introduction

In February 2014 the World Health Organization announced cancer to be the leading cause of death globally, with more than tens of millions of new cancer cases each year [2]. Many of the drugs effective in the treatment of cancer by chemotherapy are highly toxic to healthy cells and cause serious side effects. This toxicity limits the dose that can be delivered and consequently limits the efficacy of treatment. As the proportion of the World's population of elderly, who are most susceptible to cancer, continues to increase, the burden of cancer will continue to grow [2]. Annual costs associated with cancer therapy including drug development are over $40 billion worldwide [3].

One of the most common cancer treatments is chemotherapy. In chemotherapy highly potent drugs interacts with cells causing toxicity and subsequently cell death. Unfortunately, traditional chemotherapeutic agents do not discriminate between rapidly dividing normal cells and tumor cells. Their poor selectivity leads to severe systemic side effects, including multidrug resistance [4]. To circumvent the limitations associated with nonselective chemotherapeutics, researchers have developed 'smart' drug delivery systems (DDS) with a specific responsiveness to different stimuli [5-10]. Currently there is no definition of smart materials, however there is a consensus that 'smart' materials or systems respond to different bodily or external signals (pH, light, temperature), which alters their chemical, physical and structural characteristics e.g. hydrophobicity, structure, shape. By exploiting these properties it is possible to develop internally or externally activated DDS, which can transport and release drug cargo at selected location and specific time [11-13].

Typically 'smart' DDS consists of three key functionalities: (i) targeting to enhance selective binding to cancer cells – targeting is usually achieved by immobilized ligands, which recognize the cancer-specific receptors and promote cellular uptake; (ii) stimuli-responsiveness to stimuli that triggers the drug release on-demand – drug release is usually stimulated by an external signal such as near infrared light, or an internal signals inducing pH or the redox potential, and (iii) optical labeling or other diagnostic markers, which enables the direct visualization of the arrival and presence of particles on the site. This strategy is aimed to optimize the efficacy of therapies and minimize undesired side effects associated with the drug [6-10, 14].

Of all these, the ability to release the drugs in a time-controlled and site-specific manner is the most desired feature for the delivery of chemotherapeutics. The stimuli to trigger the release the

therapeutic compounds could be either intrinsic or extrinsic. Depending on the cellular homeostasis, the intrinsic mechanism includes pH, redox or enzymatic activity. Extrinsic triggers such as light, ultrasound and electromagnetic field are alternatively used to achieve the time- and site-specific delivery of drugs (as illustrated in **Fig. 1**) [11, 12, 15-18].

To this end, this review updates the most recent advances in the development of DDS, which are directed to achieve multifunctionality, enable multimodal therapy, and combine diagnosis and therapy (theranostics) in a single platform. This review demonstrates progress in the development of advanced DDS based primarily on mesoporous silica nanoparticles (MSNPs). It demonstrates the abilities to build multifunctional nanoplatforms that combine or hybridize MSNPs with molecules, drugs and other nanoparticles to obtain stimuli-responsive smart drug delivery systems. The effort carried out herein will help future designs and developments of nanocarriers that can be ideally applicable for cancer treatments.

(Insert Fig. 1 here)

2. Nanomaterials in cancer therapy

In the last decade nanotechnology allowed for the significant improvement of chemotherapy outcomes by delivering drugs locally and releasing them in finely controlled manner. Nanomaterials, i.e. nanoparticles, enable us also to overcome one of the most significant challenges in drug delivery – solubility of hydrophobic anticancer drugs. Low aqueous solubility of drugs limits the ability for intravenous delivery, which is preferred administration route for many anticancer drugs. Furthermore, nanomaterials may enhance the drug uptake by specific cells, thus achieve the same therapeutic effects with lower drug dose. The application of nanoparticles in cancer treatment has been investigated not only to enhance therapeutic efficiency and minimize adverse effects but also to lower the socio-economic burden. Despite many successes with approaches that employ nanomaterials, there is a continuous need to improve further our ability to combat cancer through the development of advanced systems that combine different materials, their functionalities and enhance synergistically therapeutic efficacy.

Nanocarriers for drug delivery can be categorized into two groups, organic and inorganic; both of which have been widely researched for the delivery of anticancer drugs (**Table 1**). Some

organic nanoparticles, such as liposomes and polymeric micelles, have been approved by FDA and are clinically used, while most of the inorganic nanocarriers still remains in the preclinical development stage [19]. *Liposomes* are approximately 100 nm colloidal spherical vesicles with an aqueous core surrounded by a phospholipid bilayer, which consists of hydrophobic tails and hydrophilic heads [17]. They are able to encapsulate both hydrophilic and hydrophobic agents within the aqueous core and lipid bilayer [18]. PEGylated liposomal anticancer agent, Doxil was approved by the FDA, due to its longer half-life in the blood stream and its ability to accumulate in tumour cells *via* enhanced permeability and retention (EPR) effect [47]. However, the undesirable dermatological adverse effects of Doxil, such as palmareplantar erythrodysesthesia, prove its lack of target specificity [48]. *Dendrimers* have well-defined hyper branched globular structures with sizes ranging from 1-100 nm [19]. Due to their synthesis process, dendrimers are relatively more stable in the blood stream compared to other organic molecules that are formed by self-arrangement [49]. Hydrophobic drugs can be loaded onto the surface of dendrimers *via* covalent bonding, while hydrophilic agents are encapsulated into the core or absorbed into the surface of dendrimers [21]. In aqueous medium, amphiphilic co-polymers are self-assembled, forming a core-shell structure, called a polymeric micelle [24]. The interior hydrophobic area allows lipophilic therapeutic agents to be loaded due to hydrophobic interactions, as well as chemical and electrostatic interactions [50]. The hydrophilic outer shell protects a cargo inside the core from chemical interactions with body fluids and rapid clearance [50]. The advantage of polymeric micelle is its smaller size (5-100 nm) compared to other nanoparticles [24]. Doxorubicin-loaded urea- or acid-functionalized PEG-polymeric micelles exhibit good drug loading capacity and release the drug sustainably, as the acidic functional groups could bind with the amine group of doxorubicin [51].

(Insert Table 1 here)

Beside chemotherapy, cancer is treated using hyperthermia (often enabled by nanoparticles) and radiotherapy (enhanced by nanoparticles). Currently, a global shift in cancer research towards multimodal therapies is observed [1]. By combining two or more modes of treatment or bioimaging, which work synergistically, significantly improved efficacy and reduce side effects can be expected. To enable multimodal therapy advanced nanomaterials are being developed and they include both inorganic and organic materials: nanogels, stimuli-responsive polymers, proteins and lipids, as well as

silica based materials. In fact, often these materials are combined together and are developed as composites or hybrids to enable multiple functionalities – multifunctional materials and particles.

For examples nanogels made of natural and synthetic materials such as: ovalbumin, pullulan, hyaluronic acid, methacrylated chondroitin sulfate and chitosan, poly (N-isopropylacrylamide), poly (Nisopropylacrylamide- co-acrylic acid) and poly (ethylene glycol)-b-poly (methacrylic acid), has been shown to be effective in delivering anticancer compounds such as doxorubicin, curcumin, 5-FU, and Cisplatin [20-22]. Advantages of using gels are that they are made of biocompatible materials, they can be functionalised with targeting molecules, and several of them is stimuli-responsive. Responsiveness to stimuli opens up the ability of controlling the drug release. To trigger the release from these materials both internal and external stimuli can be used, and the most commonly used triggers include: pH (e.g. chitosan and ovalbumin), temperature (e.g. triblock copolymer composed of poly(ethylene glycol) and poly(ethyl ethylene phosphate)), redox (copolymer that contains oligoethyleneglycol (OEG) and pyridyldisulfide (PDS)), magnetic/electromagnetic filed (e.g. nanogel-coated iron oxide nanoparticles (poly(ethylene glycol) methyl ether methacrylate (PEGMA) at Fe_3O_4), and light (e.g. amphiphilic glycol chitosan−onitrobenzyl succinate conjugates) [23].

In advanced drug delivery systems, inorganic nanoparticles are typically used, and because of their chemical, physical and structural characteristics, they enhance or support specific functionality of organic materials. At the same time, inorganic materials, which are more chemically stable [24] and their raw materials are accessible at low cost [19], can be used as ‘standalone’ DDS. Moreover, relatively simple chemical modifications can provide multifunctionality of these systems and extended their application for both diagnosis and therapy [19].

For example, *metallic inorganic nanoparticles* (e.g. iron oxide, gold nanoparticles) have been exploited to develop externally stimulated DDSs where localisation and controlled release of the drug is achieved using external signals [25, 26]. Super-paramagnetic iron oxide can be directed to targeted tumour cells using magnetic field and achieve the accumulation of the nanoparticles in desired location. By exposing these nanoparticles to the focused electromagnetic filed, the relative oscillations of the nanoparticles generate heat (thermal energy) leading to hyperthermia and subsequent cell death [27]. Similarly, gold and titanium dioxide, which are photosensitive, respond to external signals (i.e. light) and they convert light energy into heat or oxidation free radicals, resulting in increased

cytotoxic [28, 29]. In addition, they have been used as contrast agents for early detection of disease or diagnosis of the treatment effects.

Another subgroup of inorganic nanoparticles, which receives increasing popularity in drug delivery, is *mesoporous silica nanoparticles (MSNPs).* Unique architecture of MSNPs resulting from highly mesoporous structure makes this class of particles ideally positioned for drug delivery – large quantities of drug molecules can be stored in pores (reservoirs). MSNPs are considered biocompatible and cause significantly lower cytotoxicity at high concentration when compared to other inorganic nanomaterials. They also exhibit thermal stability that can is often advantages over organic nanocarriers [19].

3. Intrinsic potential of MSNPs

3.1. General aspects of MSNPs as a delivery system

Since the introduction of highly ordered mesoporous silica materials, called mobil crystalline materials (MCM-41), by Mobil researchers in 1992 [30], silica based materials have attracted significant attention, in particular in biomedical applications such as drug delivery. However, MCM-41 lacks biocompatibility and the internalization into cells is very limited due to its micrometre size [31]. To circumvent these limitations and enable their application in drug delivery, a 'downgraded' (nanosize, 50-200 nm) version of MCM-41 has been developed and is called mesoporous silica nanoparticles (MSNPs) [32].

The unique porous, honeycomb-like architecture of MSNPs provides large surface area (>700 m^2/g) [30] and high pore volume (>1 cm^3/g) [33], which are both highly desired for drug delivery and which allow loading large amount of drug into their structure [34]. In addition, pore diameter can be tuned during the synthesis, empowering MSNPs to have controlled release and to load agents with various sizes [34]. Compared to organic nanomaterials/nanocarriers, MSNPs can protect drug cargo more reliably in physiological aqueous solutions. This helps evade uncontrolled pre-leakage of therapeutic agents prior to reaching target site [34]. Due to abundant negatively-charged silanol groups (SiO^-) at physiological pH on the surface of MSNPs [30], the functionalization of MSNPs with various organic molecules can also be achieved. To minimize opsonisation, MSNPs can be decorated with positively charged molecules such as PEG [35]. While, to achieve active targeting, selected

ligands (e.g. folic acid) can also be tethered to the surface and subsequently bind to the specific, over-expressed, receptors on the target tumour cell [36].

MSNPs have shown superior biocompatibility over other inorganic nanoparticles [37], with toxicity only observed at concentration as high as hundreds of μg/mL *in vitro* [31], and at dosage above hundreds of mg/kg in mice [35]. MSNPs can dissolve under physiological conditions and be absorbed by the body or eliminated *via* renal system without considerable toxicity [30]. However, biocompatibility, biodegradation and mechanism of excretion of MSNPs need to be further evaluated since physiological complexity may affect the pharmacokinetics and pharmacodynamics of MSNPs [36].

3.2. MSNPs in cancer therapy

One of the major challenges in the development of carriers for anticancer drugs is the ability to load relatively large amount of therapeutic into vehicles and release them locally, on demand and sustainably. Mesoporous silica-based materials characterise with very large surface area (pore volume), which provides the ability to load significant amount of drug into a single particle – mesopores act as drug reservoirs. The effectiveness of mesoporous silica to deliver metalocompounds has already been demonstrated by Perez-Quintanilla *et al.* [38]. Titanocene complexes used in cancer treatment were conjugating to the mesoporous silica and higher cytotoxicity of these complexes than organic drug conjugated to the silica was observed. The conjugation of metalocompounds and some of the drugs to silica is possible because of the abundance of silanol groups (acidic silanol groups or the reactive siloxane bridges) on the surface, which can react with chlorine atoms. Reported loading efficacy was ~1.3%, however particles did not target specific site and were not stimulus-responsive. Interestingly, authors suggested that to be able to compare the effectiveness of different systems Q50 (the number of particles required to reduce normal cell growth by 50%) and M50 (quantity of material needed to inhibit normal cell growth by 50%) should be reported. It was pointed that M50 is more precise measure of cytotoxicity due to the uncertainty of particle size measurements with different techniques.

Mesoporous silica has also been shown effective in delivering cisplatin prodrug [39] that typically shows limited internalisation by cells. The Pt(IV)-based prodrug has lower toxicity in physiological environment than cisplatin, but when the prodrug is internalised by cell the activity

similar to that of cisplatin is obtained due to chemical reduction – cellular environment is highly reductive. This feature makes the use of prodrug very attractive in cancer treatment and it can lead to decrease in adverse reactions. In addition, the presence of two additional coordination sites makes it possible to functionalise the molecules and consequently overcome the solubility problem. Thus, Pt(IV)-based prodrugs are considered as a stimuli-responsive molecules and when combined with mesoporous silica their uptake by cells was significantly increased and it was shown that IC_{50} was 63 times lower than that of cisplatin. Mesoporous silica has been also shown to be effective in delivering hydrophobic drug camptothecin [40]. Silica was able to store ~80 nmol of the drug per 50 mg of the particles. Important finding in this work was that the drug remained in the pores when transported to cells in the media, and it was released primarily in hydrophobic regions of cell compartments and induced cell apoptosis. Therefore, it was confirmed that mesoporous silica is effective to deliver hydrophobic drugs, which otherwise could not be deliver intravenously.

To further increase loading capacity of drugs as well as control their release different types of hollow core and double layer mesoporous silica systems were developed. The important feature of the hollow core structures is that central part is capable of storing large quantities of drug, while its release rate can be controlled by the thickness of the shell and pore size. Chen *at al.* have demonstrated that by fabricating double-layer structure with hollow core it was possible to (i) significantly increase drug loading capacity (up to ~17%) and, (ii) control the rate of drug release [41]. These advanced structures were fabricated by selective etching of the core from particles composed of solid silica coated with two layers of mesoporous silica.

The key feature of mesoporous silica systems that makes them particularly useful for drug delivery i.e. for hydrophobic drugs, is their hydrophilicity. Hydrophobic/hydrophilic nature of drug and silica is similar to a metastable oil-in-water emulsion, where mesoporous silica shell represents here the interface between the oil (drug) loaded into the hollow core and the outer aqueous environment. In this way hydrophobic drugs are most likely to partition to the hollow core of the particles. More importantly, the drug will not be released into aqueous media (in the blood stream) but may only diffuse out slowly due to the concentration gradient, which can prevent premature and undesired drug interactions with healthy cells. Once the drug-loaded particles are uptaken by cells and they reach hydrophobic intracellular environment, the drug is released effectively (washed out) and results in cell

death.

Similarly to the other drug delivery systems, there is a large possibility for the silica nanoparticles to interact with human serum proteins (HSP) and phagocytes, which may reduce their efficacy in delivering drugs. One of the well-established approaches to prevent unspecific binding of the carriers to all cells is PEGylation. He *et al.* has demonstrated that both HSP binding and phygocytosis is related to the molecular weight of PEG. Minimal binding of HSP (2.5%) was observed for PEG-modified silica nanoparticles that characterise with molecular weight 10k and chain density 0.75% [41]. For nonPEGylated silica nanoparticles binding was as high as 18.7%. PEG-ylated silica nanoparticles showed also significantly lower phagocytosis (0.1%) than observed for unmodified particles (8.6%) [41].

Further vital part of effective cancer treatment is the delivery of the drug only to the targeted cells and tissues. Targeting is typically achieved using molecules (e.g. folate, mannose, hyaluronic acid, arginine-glycineaspartate (RGD), and lactobionic acid.) that can specifically bind to the receptors expressed on the cancer cell membrane. One of the important targets expressed on the cell membrane is asialoglycoprotein receptor (ASGPR). ASPGPR binds and internalize galactose or galactose-derived complexes (i.e. lactose – glucosylgalactose disaccharide) *via* receptor-mediated endocytosis. Lactose as low cost, nonimmunogenic, stable, and easily modifiable compound has been used to functionalise silica-based nanoparticles and deliver docetaxel. Quan et.al. showed that lactose-modified mesoporous silica particles targeted effectively ASGPR and were internalised by energy-depended mechanism, predominantly via clathrin-mediated endocytosis [42]. Subsequently, significantly increased cytotoxicity of functionalised particles was demonstrated, which resulted from upregulated uptake of the particles and the release of the drug within the cell.

Taken together, by combining different modes of treatment (chemotherapy, radiotherapy, hyperthermia), phototherapy, functionalization (targeting) and stimuli-responsiveness (heat, pH, redox) of different materials raises tantalising possibility to create hybrid systems, which are likely to significantly improve efficacy of cancer treatment and, equally importantly, reduce undesired side effects. In such advanced hybrid systems, mesoporous silica plays a pivotal role and allows storing and delivering the drug.

4. Multifunctional and smart MSNPs for DDS

Intrinsic properties of MSNPs are ideally suited for their use as DDS and spurred studies on combining and hybridizing of MSNPs with other types of nanomaterials to provide multifunctionality, which merges therapeutic and diagnostic use, as well as stimuli-responsiveness. When drug molecules are physically adsorbed to the channels of mesoporous MSNPs, they may show premature and immediate release after administration [43-45]. To overcome this undesired release and to enhance therapeutic efficacy MSNPs are combined with other materials (**Fig. 2**) [1, 46]. The combination of MSNPs with stimuli-responsive metallic nanoparticles emerges as one of the most promising hybrid system for drug delivery. It also provides diagnostic capability, as well as the ability to co-administer anticancer drugs with hyperthermia – multimodal therapy.

To achieve eradication of tumors, anticancer drugs must be administrated systematically at high concentrations. However, systemic administration of high doses of chemotherapeutics causes severe side-effects due to the nonspecific uptake of the drug by healthy cells in tissues and organs such as liver, kidney, bone marrow and heart [47]. Therefore, controlled and sustained delivery of the drugs with MSNPs is in high demand. The development of methodologies to cap the pores using different nanomaterials, known as ‘‘gatekeepers’’, was a significant advancement of MSNP-based delivery systems. When mesoporous are blocked, the drug molecules are unable to leach out, and uncontrolled and premature release is prevented. Together with this blocking action, gatekeepers sense the environmental signals that can trigger pore opening. This opening is achieved only when specific stimuli (e.g. pH, temperature [35], and redox [48]) is present and it has capability to remove gatekeepers, which then allows the drug to be released.

(Insert Fig. 2 here)

4.1. pH controlled drug release

Some of the human tissues under pathological conditions (e.g. cancer, inflammation), as well as endosomal cell compartments, are more acidic (lower pH) than healthy tissues and human plasma. Differences in pH of physiological and pathological tissues as well intracellular environment is an attractive stimulus that could be used to modulate material properties and which can be utilized to obtain specific reactions e.g. the control of the drug release [1, 14, 49].

When MSNPs are used intravenously to deliver drugs there is some likelihood of the drug to be eluted from the pores before they reach the target. However, when nanoparticles are internalised by cells *via* endocytosis, endosomal vesicles are formed and travel into the cytoplasm and fuse with other vesicles and it is the most desired for the drug to be eluted at this point. Importantly, blood and intracellular environment have different pH, which could be utilised to control elution of the drug [13]. In both situations it is preferred to close the pores and to be able to open them only when pH reaches lower values (acidic) associated with cancerous cells. Therefore, to enable the control of the drug release with pH, different classes of pH-sensitive molecules can be used as gatekeepers and cap the pores of MSNPs [50].

Therefore, to enable the control of the drug release with pH, different classes of pH-sensitive molecules can be used as gatekeepers to cap the pores of MSNPs [50]. Four major molecular strategies of the pH-responsive MSNPs have been developed, as illustrated in **Fig. 3a**. Most anticancer agents can be bonded with negatively charged MSNPs *via* electrostatic interactions at the physiological pH, due to their weak basic nature [51]. Since the weak basic drug is protonated at weak acidic conditions, the link between drug and MSNPs is cleaved, and results in drug release [14, 51]. The pore surface of MSNPs can become more negatively charged by functionalization with an acid-liable polymer, and it can reduce uncontrolled release in blood stream when compared with unmodified MSNPs [52]. The amount of the doxorubicin (pKa=8.3) released at pH=7.4 from carboxylated MSNPs and free MSNPs were respectively 43 % and 68 % after 12 h [51].

Another approach involves binding the drug into MSNPs through acid-cleavable chemical linkers, e.g. hydrazone and acetal [53-55]. Molecules loaded into the nanoparticles were shown to retain within their pores at neutral pH and the release was triggered at lower pH (**Fig. 3b**). The release profile was strongly dependent on the cleavage of the acetal linker and increased with the decrease in pH. This could suggest that drug release could be enhanced in *in vivo* conditions when nanoparticles reach cancerous cells or inflamed sites, which both characterise with lower pH [53-55].

To minimise the release of the drug molecules, inorganic pore capping materials, including gold [56] and Fe_3O_4 nanoparticles [57], can be used and link to the MSNPs through reversible, pH dependent boronate ester bond. This bond is hydrolyzed under acidic pH and the nanoparticles are cleaved and open the pores. Chen *et al.* [58] developed a pH-responsive release system based on

DNA nanoswitch that links gold NPs to MSNPs. In this system, the hybridization and dehybridization of DNA strands were controlled by pH of aqueous medium allowing opening and closing of the pores [58]. The fluorescence intensity of the solution demonstrated reversible, conformational changes of DNA obtained by the adjustment of the pH between 8.0 and 5.0 using either 1 M HCl or 1 M NaOH. Under basic conditions (pH = 8.0), no release was observed. When the pH value was adjusted to 5.0, the fluorescence intensities of DNA in solution increased rapidly, confirming that the AuNPs unblocked the pore openings. Importantly, the on–off switching can be repeated several times by sequential adjustment of pH between 8.0 and 5.0 (**Fig. 3b)**. This result strongly suggested that the mechanisms of opening and closing of pores was reversible and that the release of the drug cargo from MSNPs can be controlled by pH [58].

Park *et al.* [59] demonstrated further that molecules loaded into MSNPs could also be released in controlled way using pH sensitive polyethyleneimine/cyclodextrin (PEI/CD) polypseudorotaxane motif. When mesopores were loaded with calcein and then blocked by threading CD onto surface-grafted PEI chains at pH 11, the drop in pH to 5.5 induced the release of calcein molecules from the pores. The release was enabled by the reversible dethreading of CD from the PEI chain and subsequent pore opening. Similar approach, based on pH-sensitive CD nanovalves, was developed by Zink *et al.* who demonstrated the ability to control effectively drug release by pH-controlled pore opening [12, 60, 61]. In other approach, noncovalent interaction between *β*-cyclodextrin caps and the aromatic amine stalks were used to block nanopores and trap molecules. Lowering the pH led to the protonation of the amine stalks and the discharge of *β*-cyclodextrin. Molecules loaded into the pores could then be released [49, 62, 63].

Recently, MSNPs functionalised with dissoluble ZnO quantum dots (QDs) 'nanolids' have also shown their potential as pH-responsive nanocarriers [64]. When the release of the doxorubicin from the MSNPs capped with ZnO was examined at different pH (**Fig. 3c),** no release was observed at physiological pH (7.4). In contrast, fast release of DOX was observed at pH 5.0 and it was consistent with dissolution of the ZnO nanolids in the acidic environment [64]. The drug release reached plateau at 0.026 mmol/g within 5 h. Although the dissolution of ZnO nanolids at pH 5.0 was confirmed, the drug release kinetics was also studied at pH 2.0 to attenuate the electrostatic interaction between the drug molecules and the MSNPs. The ZnO QD nanolids not only prevent undesired drugs release in

physiological pH but they showed some cumulative cytotoxic effect on carcinoma cells. However, their cytotoxicity towards normal cells or tissues has not been presented, which remains a key issue.

Moreover, a pH-responsive MSNPs DDS based on the interaction of coordinated metal ions and the corresponding ligands was reported [65]. The formation of these conjugates is possible because both metal ions and protons (H^+) are Lewis acids and both are likely to compete for ligands (Lewis base). Here, the coordination bonds of a metal ion and its ligand is sensitive to external pH. Similarly, the modification of MSNPs surface with chitosan film has been another 'smart' design to control drug release with pH [66-68]. At high pH, chitosan undergoes shrinkage induced by the deprotonated amino groups. By decreasing the pH approximately to the isoelectric point of chitosan, it is possible to reprotonate the amino groups. The electrostatic repulsion between chitosan and the MSNPs matrix enabled the drug release, which was also achieved at different time points by the modulation of pH.

(Insert Fig. 3 here)

4.2. Temperature responsiveness

Temperature is another stimulus that may be used to trigger the release of molecules from MSNPs (**Fig. 4a)**. It has been shown that the local temperature in many tumors is slightly higher than normal body temperature. Motivated by this phenomenon, thermo-responsive polymers were used as gatekeepers on MSNPs [35]. A common temperature-responsive polymer that could be used for such purposes is poly(N-isopropylacrylamide) (PNIPAM) [27]. The volume of PNIPAM can be changed in aqueous environment at the lower critical solution temperature (LCST) [69]. Below the LCST PNIPAM chains are hydrated and extended, and when tethered to MSNPs it prevents the escape of the molecules from the pores. While the shrinkage of PNIPAM chains, which occurs above the LCST, leads to the pore opening and release of the drug [35]. Pure PNIPAM has LCST around 32°C that is not suitable for the majority of drug delivery applications due to the fact that body temperature is higher, which would keep the pores continuously open. To alter the LCST of PNIPAM, co-polymerization with other monomers, such as acrylamide [70, 71] or N-isopropylmethacrylamide, was done and it resulted in increase in the LCST to ~37°C [72, 73]. Using co-polymerized PNIPAM-based temperature-responsive drug delivery system, the release of drugs was observed at temperatures higher than 37°C. Besides thermo-sensitive polymers, other temperature-sensitive materials,

including lipids or DNA, has been utilized. Schlossbauer and co-workers demonstrated that by attaching double-stranded DNA to MSNPs and increasing temperature above melting point of DNA it was possible to control the release of fluorescein from the pores [74] (**Fig. 4b**).

The temperature increase can also be achieved by external stimuli (e.g. magnetic field, light) that interact with inorganic nanoparticles that are incorporated or attached to MSNPs. One interesting example is the use of the combination of iron oxide nanoparticles (IONPs) and PNIPAM as the gatekeepers. The exposure of the system to external electromagnetic field induces increase in the local temperature around iron oxide nanoparticles, which subsequently cause the phase transition of thermo-responsive PNIPAM and enables the drug release. More recently Baeza *et al.* has developed a novel nanodevice capable of controlling the release of small molecules and proteins in response to an alternating magnetic field [75]. This device is based on MSNPs with IONPs encapsulated inside the silica matrix and decorated on the outer surface with a thermo-responsive copolymer, PEI/NIPAM. The polymer structure was designed to act as temperature-responsive gatekeeper that close the drugs loaded pores, as well as to attract proteins to the polymer shell by electrostatic or hydrogen interactions. Such design prevented uncontrolled release of the drug at low temperatures (~20°C) and enabled the released of entrapped molecules when the temperature exceeded 35-40°C [75].

(Insert Fig. 4 here)

4.3. Redox-potential control

Living tissues, intracellular and extracellular environments exhibit different redox potentials. Because the level of glutathione (GSH) inside tumour cells is 100-1000 fold higher than within extracellular milieus, a natural redox potential can be generated [35]. These differences in redox potential may be utilized to trigger release of drug from the particles within the intracellular compartment of cancerous cells (internal trigger). Similarly to pH-responsive system, redox potential-responsive release systems have been developed, and used different nanocaps including: CdS [76] Fe_3O_4 [77] or gold nanoparticles [78] (**Fig. 5a)**, as well as biomolecules, covalently linked to the MSNPs. Disulphide bond is one of the typical redox-responsive linkers between nanocaps and MSNPs [79]. At high intracellular GSH concentration, the disulphide bridge is cleaved, forming two thiol groups at the

targeted tumour site, since GSH can act as a reducing agent [79]. At the same time the nanocap-MSNPs links are likely to be maintained in the blood [79].

Several *in vitro* studies have explored disulphide-reducing agents such as dithiothreitol (DTT) and mercaptoethanol to verify redox-potential mechanism. For example, Liu *et al.* [80] used cross-linked poly(N-acryloxysuccinimide) attached to the MSNPs pore entrances. The presence of DTT cleaved the disulphide bond of the cystamine, causing the disruption of the polymeric network and led to the redox potential-triggered drug elution. More recently, the immobilization of collagen on the outer surface of MSNPs by disulphide bonds, which can be cleaved with various reducing agents, has been demonstrated [81]. In this approach, the surface of the MSNPs was first functionalized with 3-aminopropyltriethoxysilane that resulted in NH_2-MSNP, which was then reacted with succinic anhydride to produce COOH-MSNP. Subsequently, cystamine was used to prepare the conjugate between the disulfide bond linker and MSNP (linker-MSNP). Fluorescein isothiocyanate (FITC) was utilized as both model drug and site marker for intracellular tracing of MSNPs. The linker-MSNP/FITC was further covalently coupled with collagen and attached to the MSNPs. Finally, Lactobionic acid (LA) was grafted to the collagen-capped MSNPs to produce a cell-specific targeting moiety LA-Col-linker-MSNP [81]. DTT was used as external stimulus to trigger the redox responsive release of FITC in order to investigate the controlled release behavior of LA-Col-linker-MSN. The FITC-loaded LA-Col-linker-MSN exhibited around 6.5% release within 2 hours, indicating good end-capping efficiency (**Fig. 5b**). This phenomenon could be ascribed to the loosening net structure of end-capping collagen molecules and partial physical degradation. In contrast, around 80% of FITC was released from LA-Col-linker-MSNP within 2 hours after addition of DTT, which suggested good response to DTT. This result showed that the disulfide linkages between collagen and MSNPs were cleaved/disrupted as a result of redox response to DTT (**Fig. 5b)** [81].

Moreover, other inorganic nanoparticles, including gold nanoparticles (AuNPs), QDs and IONPs, have also been tethered to MSNPs by disulphide bonds and showed similar successful redox-driven outcome – pore opening. For example, QDs, which characterize with ultrafine sizes and large surface area for functionalization, were shown to be particularly effective to close the openings of mesopore channels of MSNPs [76]. Lai *et al.* has demonstrated that by using CdS NPs linked to the MSNPs surface it was possible to control the release of drug molecules [76]. The presence of disulfide bonds

in the threads connecting the CdS NPs to the MSNP particles allowed the CdS caps to be dislodged in the presence of a disulfide-reducing agent, such as DTT or mercaptoethanol (ME). The CdS-MSNP system incorporated the vancomycin and ATP molecules effectively; furthermore, the addition of DTT and ME triggered rapid releases of those molecules [76]. The iron oxide NPs (IONPs) have also been used to close pore openings. The mesoporous nanorods were functionalized with 3-(propyldisulfanyl)propionic acid, loaded with fluorescein dye and capped through an amide linkage between propionic acid on the surface and 3-aminopropyltriethoxysilyl-functionalized IONPs. The disulfide bonds between the nanorods and the IONPs are labile and can be cleaved with disulfide reducing agents such as DTT and dihydrolipoic acid (DHLA) [77].

(Insert Fig. 5 here)

4.4. Biomolecular triggering

Biomolecules, which are typically biocompatible and biologically active, become more often used to enable drug release as they can respond to internal, bodily stimuli. Amongst different classes of biomolecules, enzymes, glucose, antigens and "aptamer-targets" are the most attractive release triggers [82]. **Fig. 6a** illustrates the scheme of 'smart' drug delivery actions of MSNPs triggered by these biomolecules.

(Insert Fig. 6 here)

The enzyme-responsive nanogates are an interesting strategy to block the pores of MSNPs due to the anomalous increase of enzymatic presence or activity in some unhealthy tissues. Climent *et al.* reported that $[Ru(bipy)_3]^{2+}$ dye-loaded polyclonal antibody capped mesoporous silica showed the ability to control opening and closing mesopores in the presence of its specific target antigen, sulfathiazole [82]. The external surface of mesoporous silica nanocarrier was functionalized with hapten, (4-(4-aminobenzenesulfonylamino) benzoic acid, which can be recognized by a specific antibody so that they bind to two antigen-binding sites of the antibody that were capped on the mesopore [82]. Once antibody-capped mesoporous silica matrix was exposed in the presence of sulfathiazole (STZ), the antibody was dissociated from MSNPs, releasing cargo stored inside of MSNPs [82]. The difference in release in the presence and absence of STZ is displayed in **Fig. 6b** [82]. The solid MSNPs show poor release profile (curve 1) in absence of STZ, whereas, in the

presence of 1 ppm STZ (curve 2) significant release was observed and confirmed the release of the dye; 95% of the maximum release of the entrapped molecules was observed after 2 h. Additionally, on-demand release of the molecules was demonstrated and achieved by adding sulfathiazole (1 ppm) at certain time points (curve 3) [82]. More recently, Bein *et al.* attached avidin caps on biotinylated MSNPs [83]. The addition of the protease trypsin resulted in the hydrolysis of the attached protein avidin and the release of the entrapped molecules. Martínez-Máñez *et al.* described the capping of MSNPs with lactose and the selective uncapping in the presence of enzyme β-D-galactosidase [84]. Very recently, multi-enzyme-responsive capped MSNPs have been developed using bulky organic moieties containing amide and urea linkages to block the mesopores [85]. Departure of the loaded cargo takes place upon addition of amidase and urease. Amidase induced an immediate, yet not complete, release of the cargo.

Conventional glucose-responsive insulin delivery systems suffer from the decrease of insulin with repeated cycles. Therefore, the use of glucose-responsive MSNPs seems a very attractive strategy for the treatment of diabetes. Zhao *et al.* [86] developed a glucoseresponsive MSNPs-based double delivery system for both insulin (Ins) and cyclic adenosine monophosphate (cAMP) with precise control over the sequence of release. Therefore, the presence of saccharides, such as glucose, would trigger the release of both G-Ins and cAMP from MSNPs. Several saccharides were tested as release triggers, including fructose, glucose, galactose, mannose, lactose and maltose (**Fig. 6c**). Among different saccharide triggers, the release of G-Ins indeed showed a strong preference for fructose, followed by glucose. Observed high selectivity for fructose is consistent with other reported monoboronic acid-based sensors for saccharide recognition [86]. Similarly, the uncapping of FITC-G-Ins and release of cAMP was achieved with glucose (**Fig. 6c)**. In PBS (pH 7.4), the cAMP-loaded FITC-G-Ins-MSN exhibited less than 10% release in the absence of glucose trigger, suggesting a good capping efficiency of FITC-G-Ins. The kinetics of cAMP release triggered by 50 mM glucose at pH 7.4 and 8.5 showed similar diffusion-controlled kinetic profiles. Specifically, ~80% of total release was obtained within 20 h (**Fig. 6d**) [86]. This double-release system set up a new model for self-regulated insulin-releasing devices.

A very innovative and interesting strategy to develop MSNPs equipped with gate-like scaffolding use highly specific antibody-antigen interactions as a powerful switchable method to develop tailor-

made MSNPs for controlled release. Climent *et al.* reported the functionalization of the pore of MSNPs with a certain hapten was able to be recognized by an antibody that acts as a nanoscopic cap [82]. The opening protocol and delivery of the entrapped cargo was related to the highly effective displacement reaction involving the presence of the antigen to which the antibody is selective.

Nucleic acid aptamers consist of single stranded short oligonucleotide sequences are used to bind to specific targets with high affinity and specificity [87]. Aptamers, i.e. DNA aptamers, are easier to obtain, more stable to biodegradation, less susceptible to denaturation and more flexible to modification than antibodies, which make them perfect candidates to design new aptamer–target-responsive MSNPs for nanomedicine [88]. One of the first 'smart' mesoporous nanosystems based on aptamer–target interactions consisted of MSNPs of which pores were capped with AuNPs modified with adenosine triphosphate (ATP) aptamer (**Fig. 6e**) [89]. The presence of the aptamer–target, *i.e.* ATP molecules, provokes the removal of AuNPs by a competitive displacement reaction, allowing molecules to be released. To determine the ability of controlling release from an aptamer-functionalised MSNP-Au system, fluorescein isothiocyanate (FITC) dye was loaded into the pores by soaking MSNP in a FITC (MSNP-FITC) solution in PBS (pH 7.4). To examine the capping efficiency, FITC loaded MSNP-Au samples were first dispersed in PBS solution without target molecules [89]. The intensity of released FITC was essentially constant, indicating no leakage of the entrapped dye molecules (curve 1), whereas the uncapped MSNP-FITC sample exhibited a rapid dye molecular transport (curve 3). This result indicated that the capping strategy was successful. The trigger release of fluorescein was investigated by the addition of ATP molecules to the MSNP-Au system (curve 2). In the presence of target molecules, the linkage between MSNP and the Au-aptamer could be dissociated through a competitive displacement reaction, and the AuNPs would be uncapped from the MSNP system. Therefore, it was expected that the release of FITC would be sensitive to the ATP molecule [89]. More recently, Ozalp and Schafer developed switchable controlled DDS using aptamers as nanovalves [90]. This reversible aptamer-based nanogvalves function could provide novel trigger systems for any desired biological stimulus in drug delivery applications.

Liu *et al*. also developed advanced matrix metalloproteinase (MMPs) targeted platform for liver and colon specific cancer treatment [91]. A PLGLAAR (Fmoc-6- aminocaproic acid-Pro-Leu-Gly-Ala-Arg-6-aminocaproic acid) peptide substrate, sensitive to MMPs, was incorporated within the amino

functionalized mesoporous silica particles. BSA was used as an end-cap for sealing the pores. Finally, as a targeting ligand lactobionic acid was conjugated onto the system. As the nanoparticles reached the tumor site, MMPs specific to liver cancer cleaved the peptide sequence between leucine and glycine facilitating the release of doxorubicin at the targeted tumor site resulting in localized tumor inhibition with minimal adverse effect on the other site of the body. Use of MMPs sensitive molecule could be a potential therapeutic measure that could be undertaken for the alleviation of tumor specific to liver and colons.

4.5. Optical tuning

Light has specific physical characteristics, which can be localized in time and space. As a result, light has been used as a trigger to release encapsulated molecules from micro and nanosystems. Many researchers have successfully incorporated light-sensitive molecules into a MSNP framework to fabricate light-responsive DDS (as shown in **Fig. 7a**). The light-responsive modulation of the MSNP state can be reversible or irreversible, which usually depends on how the chromophores link to the silica nanoparticles. The isomerization of the photochromic component in a nanocarrier can usually be followed by a thermal or visible reisomerization process. UV-light in the range of 300-400 nm is generally used for the light-stimulation, while visible light (λ > 400 nm) is typically used for the initiation of the reisomerization process.

(Insert Fig. 7 here)

The azobenzene derivatives can be reversibly isomerized between a planar transform and non-planar cis form in aqueous environments under UV or visible light irradiation [92-94]. A distinctive advantage of this system lies in the reversible capping of pores, thereby enabling more complicated on-demand cargo delivery. As a proof of concept, the release of trapped dye molecules was regulated with open-close cycles *via* alternating irradiation wavelengths. As demonstrated in **Fig. 7b**, the closed state with visible irradiation strongly constrained the delivery of the Rh6G molecules [92-94]. On the other hand, a distinct release of the entrapped rhodamine dye was triggered in the open state as a result of dehybridization when the wavelength was changed to 365 nm at 120 min. After 240 min, the release of the entrapped dye was again restricted by changing to visible light (450 nm). At 360 min, UV irradiation was repeated, and further delivery of the entrapped dye occurred. Subsequent

irradiation with visible light inhibited again the release of the dye. The decreased dye release rate in each open segment is attributed to the reduced amount of dye to be delivered from the pores in each cycle [92-94]. The release process shows that the on-off switching is reversible and can be repeated several times. On the basis of the photosensitive DNA, the delivery of small molecules by MSNPs can be achieved automatically by sequential adjustment of light. This 'smart' stimuli-responsive behavior should be useful for on-demand dosing in clinical situations. An irreversible light-responsive nanosystem can generally be found in silica nanoparticles that have photocleavable components instead of photochromic ones. Upon irradiation, the light-responsive moiety would be converted into more polar species through an irreversible transformation. The chromophore o-nitrobenzyl ester (ONB) [95] that shows irreversible light-responsiveness, has been extensively applied in the UV-light initiated photocleavage reaction. The reversible or irreversible cross-linking reactions based on coumarin dimerization have also been applied to the synthesis of light-responsive MSNPs [96]. Various photoresponsive linkers, such as *S*-coordinated $Ru(bpy)_2(PPh_3)$-moieties (absorption at visible light) [97], thioundecyl-tetraethylene-glycol-ester-o-nitrobenzylethyl dimethyl ammonium bromide (TUNA) (absorption at UV region) [98] and 7-amino-coumarin derivative (CD) (absorption at visible or NIR) (**Fig. 7c**) [99], have been functionalized onto MSNPs to enable light-driven release. Precise control of the photolytic release from CD-MSNPs was demonstrated by monitoring the progress of chlorambucil release after periods of exposure to light and dark conditions, as shown in the inset of **Fig. 7c**. The distinctive "stepped" profile revealed that the drug release only proceeded under light conditions, thus realizing "light-regulated precise release". All the results indicated that the CD-MSNP based DDS could precisely control drug release by manipulating external light intensity, irradiation wavelength, and time [99].

It is notable that UV or blue light has been frequently applied in light-responsive strategies. Nevertheless, they are less suitable for *in vivo* therapeutic applications, since UV light may cause unwanted reactions, including cellular apoptosis. In addition, the rapid intensity attenuation of the short-wavelength light in tissues further limits their applications in biological systems [100]. Therefore, the irradiation with a wavelength below 700 nm, due to the insufficient penetrability (less than a few micrometers deep), was often limited to skin or external layers of organs. For this reason, UV-responsive MSNPs were usually only applied to epidermis or mucosa treatments. To improve the light

penetration in tissue, near-infrared (NIR)-triggered smart materials have recently drawn considerable attention, facilitating a better resolution in depth (more than a few micrometers) [101]. Such light-responsive systems are primarily composed of metal nanoparticles as the core, which could efficiently absorb the NIR light and convert it to heat for photothermal therapy [102]. Combined with a thermal-responsive polymeric shell or coordinated bonds, drugs could be released with increased temperature upon remote NIR light irradiation [103, 104]. Both the loading capacity of drugs and the intensity of the NIR irradiation may influence the efficiency of NIR responsive drug delivery, which has been the pivotal factor for the chemo-photothermal therapy.

The FDA has recently approved gold as a therapeutic agent for the treatment of rheumatoid arthritis, implying its safety for humans [105]. Their size range (20-500nm) allows therapeutic agent-loaded AuNPs to pass into leaky tumour vascular sites and retain in tumour cells [106]. Due to their inertness, AuNPs are stable against physiological degradation by enzymes *in vivo* [106]. Modifications of their surface with various polymers enhance active targeting ability and biocompatibility [107-109]. Localized surface plasmon resonance (LSPR) is a unique phenomenon, which is the collective oscillation of surface free electrons *via* irradiation by light, followed by the scattering and absorption of light at resonant wavelengths [107-109]. AuNPs could absorb the NIR region, which can penetrate into deep soft tissue without cytotoxic effect of UV light [106, 109]. The absorbed NIR light source is converted into local thermal energy, creating hyperthermia [108]. The NIR laser-induced plasmonic heat can elevate local temperatures above 45°C, leading to the destruction of tumour cells [110]. Using their large scattering and absorption cross sections, AuNPs have been used as an optical contrast agent for dark ground microscopy, such as photoacoustic tomography (PAT) [110]. Once PAT illuminates the AuNPs-injected sample, an acoustic signal is generated by a local thermal rise and converted into a dark background with bright sample image [105]. External photo- or magnetic-induced hyperthermia and photo-stimulated photodynamic process with co-administration of anticancer drug-loaded MSNPs have been studied as a novel dual antitumor therapy and showed greater cell death compared to chemotherapy or photothermal therapy alone [111, 112]. The efficiency of photothermal cancer treatment was examined *in vivo* using mouse model (**Fig. 7d,e**) [113]. Tumor-bearing mice were administrated intravenously with 100 µL of saline (as control) or 100 µL of 15 nM (or 9×10^{12} particle/mL) PEGylated AuNPs (called nanocages). After 72 h post injection, the tumour

on the right flank of each mouse was irradiated with an 808-nm continuous-wave (CW) diode laser at a power density of 0.7 W/cm^2 for 10 min. During the treatment, the tumours containing AuNPs were rapidly heated to temperatures over 55°C, while no detectable temperature change was observed for the control. The measurement of tumor metabolism with [^{18}F]fluorodeoxyglucose (^{18}F-FDG) positron emission tomography (PET) (^{18}F-FDG PET) imaging was performed before and after laser treatment for mice that had been intravenously injected with either saline or nanocages. Before laser irradiation, the ^{18}F-FDG PET imaging showed no significant difference between saline-injected mice (A) and nanocage-injected mice (B). At 24 h post-laser treatment, the metabolic activity in tumours of nanocage-injected mice (D) was significantly reduced as compared to that of saline-injected mice (C) (**Fig. 7e**). The normalized value was ~0.3 after irradiation for the mice injected with Au nanocages as opposed to ~1 before irradiation, indicating a decrease of metabolic activity by 70%. For the saline-injected mice, the normalized value of ^{18}F-FDG uptake was close to one before and after uptake, suggesting there is no benefit to laser treatment in the absence of Au nanocages.

Another important class of materials that are particularly useful for phototherapy are upconversion nanoparticles (UCNPs). UCNPs are rare earth nanoparticles composed of lanthanide ions such as Tm^{3+}, Er^{3+},Ho^{3+} and Sc^{3+} [114-116] and possess distinctive upconversion ladder-like energy level structures. This unique property enables them to absorb two or more lower energy photons of the NIR light and emit single high energy photon of shorter wavelength in the UV or visible region [114, 117, 118]. In addition to this, they have sharp emission band-width, long luminescence shelf life, greater photostability and light penetration depth along with lower cytotoxicity and lesser background autofluorescence [115]. These properties make them suitable for the application as a theranostics for the detection and treatment of cancer. Owing to these attributes, UCNPs were utilised for targeted photothermal therapy (PT) [118], photodynamic therapy (PDT) [119]·[120] or combination of either of these processes with chemotherapeutics [114, 121, 122] to achieve synergistic effect to combat cancer.

To fabricate UCNPs three components are essential: a host matrix, a sensitizer and an activator. Commonly, fluorides such as $NaYF_4$ [114, 117, 123], $NaGdF_4$ [124-126], $NaLuF_4$ [127-129], KYF_4 [42, 130], $NaYbF_4$ [131, 132], LaF_3 [133], CaF_2 [134-136], $KmnF_3$ [137], YF_3 [138], $KGdF_4$ [139], are used as hosts in combination with sensitizer such as porphyrin derivatives [123], Chlorin e6 [140],

phthalocyanines [141], porphycenes, zinc (II)-phthalocyanine [123] and NIR being the activator for drug release. Number of fabrication strategies such as thermal decomposition, hydrothermal or solvothermal, coprecipitation, sol gel processing, combustion synthesis, flame synthesis, anisotropic island nucleation and growth have been used for the development of some of the smart UCNPs [125, 142],[125, 143-145].

For the photothermal applications, UCNPs are used in conjunction with light absorbing agents such as gold, carbon and inorganic nanoparticles/nanomaterials. The process of upconversion generates high energy photon resulting in localized hyperthermia that leads to cell death. Whereas, in case of PDT, the combination of UCNPs with some photosensitizer moieties such as Roussin black [104], Rose Bengal [109], Chlorin e6 [140] and oxygen are used [119]. The activation of photosensitive agents occurs due to the resonance energy transfer after NIR absorption and results in the generation of singlet oxygen, reactive oxygen species (ROS) and in some cases nitric oxide. These species cause the oxidation and nitrosation-led damage of tumorous cells [118-120, 123, 141]. Most of the PDT is based on ROS mediated cell death. Recently Zhang *et al*. developed a 'smart' drug delivery platform for cancer treatment where nitric oxide was released from UCNPs (mesoporus silica coated $NaYbF_4$:Tm@ $NaYF_4$:Yb/Er core-shell structure) using NIR **(Fig. 8a)**. Photosensitive nitric oxide donor (Roussin's black) was incorporated within the mesoporous structure, which facilitated the release of nitric oxide after irradiation with NIR **(Fig. 8b)**. The release of nitric oxide lead to cytotoxic effect due to mitochondrial and DNA destruction by both oxidation and nitrosation. In addition, nitric oxide inhibits the P-glycoprotein, which is one of the proteins responsible for efflux of anticancer drug leading to development of multidrug resistant cancer **(Fig. 8c)**. Improved efficacy of chemotherapeutics was observed after the NIR irradiation suggesting the effectiveness of this novel approach. Also, in the presence of nitric oxide the efficacy of doxorubicin was found to be enhanced for doxorubicin resistant MCF cells [120], which shade the light into new approaches to treat multidrug resistant cancer.

Furthermore, Chen et al. demonstrated the synergistic PDT/PTT photo-killing effects of bovine serum albumin (BSA) modified $NaGdY_4$-based UCNPs [118-120, 123, 141]. Here, two types of dye molecules, including a photosensitizer, Rose Bengal (RB), and an NIR-absorbing dye, IR825, were

simultaneously loaded into the BSA of the UCNP@BSA. The potential of UCNP@BSA-RB&IR825 nanocomplex for *in vivo* imaging and cancer combination therapy observed in mice bearing 4T1 tumors. Upon intratumorally injection with the nanoparticles, obvious T1-weighted MR signals were observed from tumors, demonstrating the ability for multimodal imaging. Although the PTT caused by the hyperthermia induced was slightly more effective in killing cells than the PDT, the combination of both therapies induced a synergistic effect compared to the monotherapy (**Fig. 8d**). The tumor size measurement and the histological examination supported that the combined PDT-PTT treatment severely damaged the tumor, whilst the mono-therapy (PDT only or PTT only) only partially destructed (**Fig. 8e,f**).

(Insert Fig. 8 here)

Liu *et al*. has recently developed MSNPs for controlled delivery of doxorubicin using a NIR switchable UCNPs containing $NaYF_4$: TmYb core, $NaYF_4$ as shell and external coating of mesoporous silica. Azobenzene (N-(3-triethoxysilyl)-propyl-4-phenylazobenzamide) groups were incorporated in the pores of these nanoparticles followed by functionalization with TAT peptide on the surface to target specific tumor site. NIR (980 nm) exposure resulted in the release of photons in UV and visible regions leading to the photoisomerisation of azobenzene moiety. Azo molecules possess unique switchable property, which on exposure to UV photons transforms to cis form and to trans form in the visible photon range. The conversion from cis to trans form resulted in rotation-inversion mechanical motion within the mesoporous structure facilitating the release of doxorubicin in a controlled manner [116]. In another study conducted by Fedoryshin *et al.,* photocleavable o-nitrobenzyl derivative of 5-fluorouracil coupled to o-phosphorylethanolamine ligands incorporated within the MSNPs containing upconversion β-$NaYF_4$:Yb:Tm core and β-$NaYF_4$ shell coated with was explored for controlled release of 5-fluorouracil upon irradiation with NIR. Laser power controlled release of 5-FU was achieved with complete release of drug within 14 minute of NIR irradiation at a laser power of 30 mW. Drug release kinetics was dependent on the power of laser supplied where drug release was 130 μM min^{-1} at 80 mW whereas at 10 mW drug release was significantly lower accounting for 18 μM min^{-1}. [114] This smart platform may be explored for the development of laser tunable controlled and targeted therapy for cancer therapeutics.

Dual compartment Janus nanopartilces (Janus MSNPs) has also been explored for externally

activated drug delivery for cancer therapy [127]. Janus nanoparticles characterised with both hydrophilic domain (UPCNPs@silica core with mesoporous silica nanospheres as shell) and hydrophobic domain composed of periodic mesoporous organosilica (PMO). Hydrophilic drug doxorubicin was loaded within the hydrophilic mesoporous structure and paclitaxel being hydrophobic was functionalized on the hydrophobic PMO domain. In addition, to achieve biomodal switching, the radial portion of the mesoporous core was modified with the UV/visible light sensitive azobenzene molecule and outer portion of entire particle was coated with thermoresponsive phase changing material 1-tetradecanol. The combination of NIR irradiation and generated heat caused the release of drugs leading to HeLa cell death. Similarly, the energy released from UCNPs activated the photoisomerization of azobenzene and triggered the release of doxorubicin. It also caused an increase in temperature above 39°C that resulted in melting of 1-tetradecanol and releasing paclitaxel [142].

One of the key aims for advanced drug delivery systems is the ability to combine different modes of treatment in a single platform. One of the examples of such platform is mesoporous silica coated with Gd-UCNPs, which are capable of co-delivery photo- and radio-sensitive hematoporphyrin along with radiosensitive chemotherapeutic, docetaxel. Upon exposure to NIR and X-ray irradiation complete inhibition of tumor occurred and was associated with the synergy of radio, chemo and photodynamic therapeutic effect [122]. In other study, Liu *et al.* showed that single walled carbon nanotubes (SWNT) coated with mesoporous silica and modified with polyethylene glycol (SWNT-PEG-Mesoporous silica) were effective to deliver doxorubicin and induce hyperthermia when exposed to NIR. An increase in the local temperature around nanoparticles was generated by the absorption of NIR radiation by SWNT. Cumulatively, generated heat and released doxorubicin from the nanoparticles resulted in significant inhibition of cell growth [121].

4.6. Magnetic activation

In addition to pH, thermal, redox potential, and optical signals, the magnetic field could also serve as a potent stimulus to trigger the release of molecules from MSNPs. In fact, magnetic nanoparticles with a size range of 10-100 nm have been used as an external magnetic responsive multimodal DDS due to their superparamagnetic properties [46]. IONPs are the most commonly used magnetic

nanomaterials. IONPs have two main forms, magnetite (Fe_3O_4) and its oxidized metabolite, maghemite (γ-Fe_2O_3) [146]. Magnetic fields are generated by strong permanent magnets, mostly, neodymium magnets [147]. To localise the nanoparticles in the target tissues magnetic fields can be applied externally and focused on specific areas. IONPs with immobilised therapeutic agent will be then attracted to the targeted location [146]. As the strength and location of the magnetic field can be modulated, the accumulation of the nanoparticles can be controlled leading to the reduction of undesirable cytotoxic effects on healthy tissues [33]. Magnetic field gradient is affected by local resistance, caused by blood flow, and the depth of targeted area [146]. Thus, IONPs tend to be more effective at the areas of slower blood flow and near to surface [146]. IONPs are generally coated with hydrophobic polymers [148], to avoid opsonisation which subsequently increases blood circulation time of IONPs, and to provide surface for binding of drug molecules and/or specific targeting ligands [69].

Along with the potential to deliver drugs, magnetic nanoparticles are used for bioimaging and diagnostics. Magnetic resonance imaging (MRI) is the most representative clinical diagnostic modality, characterized by non-invasive, non-ionizing, real-time and cost-effective features. For soft tissue imaging, researchers commonly employ Gd^{3+} molecules as chemical contrast agents. In addition to Gd^{3+}, magnetic nanoparticles of elements such as Fe, Ni, Co, Mn, Cr, as well as their chemical compounds are also used in MRI.

Therefore, the combination of magnetic nanoparticles with MSNPs constitutes a promising alternative for drug delivery with a high loading capacity and target-specificity and magnetic properties for targeting and controlling the release. Magnetic nanoparticles can be either tethered onto the MSNPs surface via chemical linkers of coated with MSNPs resulting in a core-shell structure. Recent studies have reported on IONPs-coupled MSNPs for MRI contrast agents to monitor cancer cells and animal tumours (as schematically shown in **Fig. 9a**) [47, 75, 149-152]. However, to fully utilise the magnetic properties in combination with MSNPs Chen *et al*., developed MSNPs capped with IONPs that were link to the surface *via* thermo-sensitive polymer [149]. MSNPs were first functionalized with 3-aminopropyltrimethoxysilane (APTS) and then loaded with the anticancer drug camptothecin (CPT). The application of magnetic field removed the Fe_3O_4 nanocaps due to the physical cleavage of chemical bonds, which led to drug release. Similarly, Vallet-Regi *et al.* demonstrated that using

alternative magnetic field it was possible to open and close the pores ('on–off') repeatedly **(Fig. 9b)** [153]. In the system, oligonucleotide was used as the linker between MSNPs and IONP nanocaps, and the DNA duplex was selected to display a melting temperature of 47°C, which corresponds to the upper limit of therapeutic magnetic hyperthermia temperature range. The fluorescein-loaded particles were exposed to an alternating magnetic field of 24 kAm^{-1} and 100 kHz inside a thermostatic chamber at 37°C [153]. The particles were able to heat the environment to hyperthermic level after several minutes under the influence of the magnetic field, which was maintained until temperature stabilization of the medium (47°C). In order to assess the 'on-off' behavior of the system, after maintaining the temperature for 15 min, the particles were cooled to room temperature (20°C). Interestingly, every time the thermal stimulus was removed the fluorescein-labelled oligonucleotides were retained again within the mesoporous silica, and fluorescein detection in the supernatant was close to zero [153]. The reversibility of DNA linkage results in an 'on-off' release mechanism **(Fig. 9c)**. Moreover, the magnetic component of the whole system allows reaching hyperthermic temperatures (42-47°C) under an alternating magnetic field. This fact ensures a reversible mechanism through DNA rehybridization. While significant *in vitro* findings have been piled up, demonstrating the synergistic effects obtained with different modes of treatment, *in vivo* tests have rarely been performed.

(Insert Fig. 9 here)

4.7. Multiple stimuli-responsive gatekeepers

Multi stimuli-responsive DDS are able to respond to two or more stimuli, either in an independent or in synergistic fashion **(Table 2)**. Chang *et al.* reported the synthesis of core-shell MSNPs with thermo/pH responsive [154]. Magnetic MSNPs were used as the core and cross-linked poly(N-isopropylacrylamide- co-methacrylic acid) (P(NIPAM-co-MAA)) polymer was used for the outer shell. The thermo-responsive volume phase transition (VPTT) could be precisely regulated by the molar ratios of MAA to NIPAM and the concentration of NaCl. The amount of drug released was small below the VPTT and increased above that value, exhibiting an apparent thermo/pH-controlled drug release. In a very recent work, Chen *et al.* reported the synthesis of double stimuli-responsive vehicles by attaching self-complementary duplex DNA to the openings of MSNPs, which resulted in a cap for

trapping guest molecules [41]. The duplex DNA cap could be either denatured by heating or hydrolyzed by endonucleases, thus opening the nanopores and releasing the cargo.

Martinez-Manez and co-workers anchored polyamines on the MSNPs surface to obtain pH sensitive and anion-controllable gate-like assemblies capable of controlling the release of a ruthenium dye trapped inside the mesoporous matrix. To achieve this goal, they varied the pH value and content of certain anions into the release medium [155]. The same group also modified the pore outlets of MSNPs with boronic acid-functionalized AuNPs acting as nanocaps. These NPs were linked to the surface of saccharide-functionalized MSNPs through the formation of boronate ester bonds, which are hydrolyzed under acid conditions (pH = 3). The nanosystem exhibited an 'on-off' response because of the reversibility of the boronate bond formation. Moreover, the metallic nanoparticles could be heated by laser irradiation at 1064 nm causing a light-induced (plasmon-resonance) release due to the thermal boronate bond cleavage. Double-stimuli controlled release MSNPs could also be used as AND logic gates, as have been recently demonstrated by Angelos *et al.* [156]. In this case, two different molecular structures have been mounted on the mesoporous silica surface, azobenzene as light-sensitive nanoimpellers and pseudorotaxanes as pH-responsive nanovalves. These two systems can work separately, but only the simultaneous activation of both molecular structures achieves the release of the molecules. Such devices could not only be used in drug delivery applications, but could also perform simple logic operations.

Wu *et al*. synthesized a carbohydrate-functionalized MSNP which was capped with concanavalin A onto the cylindrical pores to achieve Rhodamine 6G controlled release by competitive binding of glucose at high concentration and decreasing surrounding pH **(Fig. 10a)** [157]. The interaction between concanavalin A and carbohydrate can be achieved in the presence of Ca^{2+} and Mn^{2+}. Rhodamine6G (Rh6G) was selected as a model drug for convenient detection of the release, because its fluorescence emission remains unchanged not only in the presence of Ca^{2+}, Mn^{2+}, and Con A but also with a change of pH from 7.4 to 1.5. With decreasing pH of the buffer, the fluorescence emission of the Con A-gated MSNP system significantly increased (**Fig.10b**), which indicated that the protein nanogates opened and the cargo was released from the MSNP pores [157]. The efficiency of release gradually increased with the drop of the pH (from 7.4 to 5.5, and then to pH 3.5 and 1.5). At lower pH Ca^{2+} and Mn^{2+} ions were dialyzed out of the protein binding pockets, resulting in removal of

the Con A proteins from the MSNP surface, in addition, the Con A tetramers disassociated into dimers and monomers below pH 5.5. Both of these factors caused the protein nanogates to open and release the molecules from the pores. The amount of released molecules was pH dependent. In the presence of glucose, the fluorescence emission of the Con A-gated MSNP system gradually increased with increasing glucose concentration because of competitive binding of glucose to the proteins which drove the removal of proteins and controlled the release of molecules (**Fig. 10c**) [157]. Thus, glucose in the normal range was not an effective release trigger because glucose has lower binding affinity than mannose and it is difficult for glucose at low concentrations to disrupt the multivalent mannose–Con A interactions. On the other hand, with high concentrations of glucose sustained and increased rate of the release of molecules from the MSNP pores was observed. The mechanism of controlled release by competitive binding is different from that of the pH-responsive release. Hence, it is has been demonstrated that carbohydrates can act as ligands and bind to the protein pockets of Ca^{2+} and Mn^{2+}, which can be removed by dialysis in the acidic condition (pH <5.5), followed by the transformation of concanavalin A from tetramer to dimer and/or monomer. Such systems that show dual glucose and pH-responsiveness can be potentially useful for both cancer and diabetes therapy.

(Insert Fig. 10 here)

(Insert Table 2 here)

5. Future perspectives

A major challenge of modern medicine is the administration of therapeutics in a more physiologically acceptable and discreet manner. In many cases, the systemic drug doses prescribed need to be high to ensure that the correct minimum dose reaches the target area. Unfortunately, a large portion of the dose interacts with healthy tissues on the way to the target, resulting in severe side effects. This problem is compounded in cancers, where the risk-benefit analysis associated with chemotherapy is often difficult because of the cytotoxicity of the drugs used. However, this scenario can be extended to other situations, where the accessibility of the drug towards the target tissue is difficult. For instance, the low blood irrigation of bone compared with most of soft tissues means that very high doses are required to be effective.

As discussed above, functionalized MSNPs have proven to be promising materials for imaging and drug delivery in cancer and beyond. In these systems, different types of molecules and therapeutics can either be loaded into the nanoporous structure or tethered onto the surface using diverse linkers. In any case, the controlled diameter, porosity, texture or chemical composition is coupled with adaptive properties such as the pH, optical, thermal, light or magnetic-stimulation for molecular-recognition. Given these functionalities, silica-based nanocarriers can serve as customizable, considerably stable, targeted drug delivery vehicles, capable of carrying sufficient cargo of chemotherapeutic or molecular agents into malignant cells, while sparing healthy cells. Current investigations, as presented in this review, have proved to be highly promising, with results indicating that the drug delivery rate, bio/chemical sensing and various stimuli-triggering can all be arbitrarily and precisely controlled. This is expected to greatly reduce or even eliminate the undesirable side effects that limit the efficacy of current cancer therapies.

It is important to target the affected regions of the body with specific pharmaceutical compounds; these drugs can be liberated in a controlled manner over time. It could be achieved by only using versatile new delivery platforms that (i) provide specific target recognition of cancer cells, (ii) substantially enhance the delivery of cytotoxic agents to the targeted cancer cells and (iii) controllably release the drug within cell compartments to maximize efficacy of the treatment and minimize the side effects. Evidently, to prepare ‘smart’ multifunctional nanocarriers, different materilsa have to be simultaneously assembled. The next generation of theranostics will likely have enhanced surface characteristics, making them more biocompatible, water-soluble or colloidal, displaying reduced toxicity and high differential uptake efficiencies. Moreover, these individual moieties have to function in a certain coordinated way to provide desired combination of selected properties. The development of multi-functional nanoscale systems for combined sensing, imaging and therapy are continuing to be active subjects of nanomedical and pharmaceutical research.

Based on the knowledge we have acquired, we anticipate that the data reported so far, regarding the biological effects of these nanomaterials both *in vitro* and *in vivo*, needs to be improved further to achieve realistic clinical needs. The chemical versatility of these non-metallic nanomaterials shall afford these nanocarriers with clinically applicable properties such as better blood circulation,

tumor-specificity, biodegradability and clearance from the animal/human body. We foresee their potential in future theranostics.

Acknowledgements

The Faculty of Pharmacy in University of Sydney for funding to support the international honours research program. A support from the Priority Research Centers Program (No. 2009-0093829), National Research Foundation, Republic of Korea.

Captions for figures and tables

Fig.1. The MSNP-based nanocarrier drug delivery system as adaptable platforms for stimuli-responsive drug delivery in cancer therapy. The time- and location-controlled drug release can be achieved by temperature, redox potential, pH gradient, photo irradiation, biomolecules, and electro-magnetic field.

Table 1. Classes of organic and inorganic nanocarrier systems.

Fig. 2 Multifunctional anticancer theranostic model. Hybrid MSNPs with gold nanorod core; irradiation with NIR increases the temperature of the particles (hypothermia) while the drug is eluted from pores; gold nanorods allow visualisation using CT when nanoparticles are accumulated in the target tissue.

Fig. 3 (a) Schematic drawing of the pH-responsive MSNPs with four major molecular designs, including acid-liable linker (i), *β*-cyclodextrin and aromatic amine stalk (ii), dissoluble ZnO QD as a nanolid (iii), and transition metal ion (iv). **(b)** Fluorescence intensity showing the pH-reversible switching of the DNA nanoswitch at pH 5.0 and 8.0 (data permission from ref. [96]) **(d)** Release profiles of ZnO@MSNPs–DOX at pH 7.4, 5.0, and 2.0 at 37 °C (data permission from ref. [102]).

Fig. 4 (a) Schematic representation of the temperature-responsive drug delivery system with MSNP, including thermo-responsive polymer coating (i) and temperature-controlled valve system (ii). **(b)** An exemplar study on valve system, where the temperature-dependent pore-opening is actioned by the double-stranded DNA linkers. Avidin proteins that are joined to the DNA by a biotin modification act as the molecular valve at the exits to the pores; FRET measurement of samples in the open and closed state (left), and the fluorescein release from samples with different length of DNA with variation in temperature (data permission from ref. [114]).

Fig. 5 (a) Schematic representation of the redox-responsive delivery system based on gatekeeper inorganic nanoparticles (QDs, IONPs, and AuNPs) caped on MSNP. **(b)** An exemplar study on

collagen-attached MSNPs by a disulfide linker followed by introduction of lactobionic acid (LA) cell targeting moiety; the release profile of FITC from the nanoparticles is responsive to the addition of DTT solution and the system shows efficient endocytosis to HepaG2 cells (empty bar; w/o cap vs. filled bar; with cap) (data permission from ref. [121]).

Fig. 6 (a) Schematic representation of the biomolecular (antigen (i), enzyme (ii), glucose (iii), and aptamer (iv)) trigger delivery system based on MSNP. **(b)** Release kinetics of dye from solid MSNP in the absence (■) and presence (▲) of 1 ppm sulfathiazole (STZ) in aqueous PBS (pH 7.5); a third curve (◊) shows the release profile of dye complex from MSNP in PBS (pH 7.5) until *t* = 70 min (indicated by the arrow in the figure), when suddenly STZ (1 ppm) is added to the solution (data permission from ref. [122]). **(c)** Dependence of FITC-G-Ins release from FITC-G-Ins-MSNP on the concentration of different saccharide triggers, and **(d)** controlled release of cAMP from FITC-G-Ins-MSNP triggered by 50 mM glucose at pH 7.4 (●) and 8.5 (▲), with control data at pH 7.4 in the absence of glucose (■) (data permission from ref. [126]). **(e)** Time course of fluorescein release from MSNP-Au in the absence (■) and in the presence of ATP (▲), and the control test for MSNP-FITC also shown in (●) (data permission from ref. [129]).

Fig. 7 (a) Schematic representation of the light-responsive (UV, visible, laser, and NIR) MSNP-based DDS, capped with (i) gold nanoparticle (AuNP), (ii) $Ru(bpy)_2(PPh_3)$, (iii) thermal polymer, and (iv) 7-amino-coumarin derivative (CD) system for controlled release. **(b)** Rh6G release profile from MSNP as a function of time, showing the reversible dehybridization/rehybridization switching by changing the UV/visible light wavelength (data permission from ref. [133]). **(c)** The drug release process from chlorambucil-grafted CD-MSN material under 420 nm light irradiation; inset is the partial progress for the release of chlorambucil from CD-MSN material under bright (ON) and dark (OFF) conditions (data permission from ref. [138]). **(d)** ^{18}F-FDG PET co-registered images of mice intravenously administrated with either saline or PEG–AuNPs, followed by laser treatment; a nanocage-injected mouse (A) prior to and (B) after treatment, and a saline-injected mouse (C) prior to and (D) after treatment; the white arrows indicate the tumors that were exposed to the diode laser at a power

density of 0.7 W/cm^2 for 10 min, and **(e)** a plot showing the ratios of laser-treated tumor to non-treated tumor for ^{18}F-FDG standardized uptake values (data permission from ref. [149]).

Fig. 8 (a-c) NO-releasing UCNP@MSNP as the NIR photosensitizing theranostic platform; (a) schematic illustration of the system for dose-controllable nitric oxide (NO) release by using photolytic Roussin`s black salt (RBS) as the NO-donors, **(b)** ON/Off behavior of the NO generation induced by 980 nm laser irradiation for different power outputs, and **(c)** cytotoxicity assay in MCF-7/DOX under different treatments (data permission from ref. [156]). **(d-f)** UCNP@BSA-RB&IR8 system enabling PDT/PTT combined tumor therapy; (**d**) IR thermal images of 4T1 tumor-bearing mice i.t. injected with either PBS or UCNP@BSA-RB& IR825 and the exposed to the 808-nm or 980-nm laser irradiation at the power density of 0.5 W/cm^2, (**e**) *in vivo* tumor growth in different groups of mice after various treatments indicated. Six groups of mice (*n* = 5 per group) were used in our experiment: 1: untreated, 2: laser only (808 nm + 980 nm), 3: injection only, 4: PDT, 5: PTT, 6: PTT + PDT. 808-nm (0.5W/cm^2, 5 min) and 980-nm (0.4 W/cm^2, 30 min) were used to separately trigger PTT and PDT, respectively, and (**f**) micrographs of H&E-stained tumor slices harvested from mice with different treatments indicated (data permission from ref. [155]).

Fig. 9 (a) Schematic representation of magnetic field-responsive MSNPs. A metal-chelate complex of gadolinium such as Gd-DTPA and manganese oxide NPs have been applied as a preferred T_1 contrast agent for MRI, while iron oxide NPs were commonly introduced as T_2 contrast agents which provided dark, negative images as the intensity of the T_2 signal increased. **(b)** DNA-linked magnetic NP-capped MSNPs demonstrating drug release mechanism driven by the DNA cleavage associated with temperature rise under an alternating magnetic field, and **(c)** temperature-responsive release curve of fluorescein from the system (data permission from ref. [190]).

Fig. 10 (a) Dual glucose and pH responsive nanocarrier. Concanacalin A capped on carbohydrate-functionalized MSNP can controlled release of rhodamine 6G in the presence of high concentration of glucose and in the acidic environment (pH < 5.5). **(b)** Release profiles of Rh6G from Con A-gated MSNP at different pH values. **(c)** Release profiles of Rh6G from Con A-gated MSNP in the presence

of different concentrations of glucose in tris-HCl buffer solution (pH 7.4) (data permission from ref. [195]).

Table 2. Stimuli-responsive MSNP-based DDS applied in cancer diagnosis and therapy - theranostics.

References

[1] Wang Y, Song S, Liu J, Liu D, Zhang H. ZnO-Functionalized Upconverting Nanotheranostic Agent: Multi-Modality Imaging-Guided Chemotherapy with On-Demand Drug Release Triggered by pH. Angewandte Chemie International Edition 2015;54:536-40.
[2] Ma X, Yu H. Global Burden of Cancer. Yale Journal of Biology and Medicine 2007;79:85-94.
[3] Hillner BE, Smith TJ. Efficacy Dose Not Necessarily Translate to Cost Effectiveness: A Case Study in the Challenges Associated With 21st-Century Cancer Pricing. Journal of Clinical Oncology 2009;27:2111-3.
[4] Dean M, Fojo T, Bates S. Tumour stem cells and drug resistance. Nat Rev Cancer 2005;5:275-84.
[5] Paciotti GF, Kingston DGI, Tamarkin L. Colloidal gold nanoparticles: a novel nanoparticle platform for developing multifunctional tumor-targeted drug delivery vectors. Drug Development Research 2006;67:47-54.
[6] Trewyn BG, Giri S, Slowing II, Lin VSY. Mesoporous silica nanoparticle based controlled release, drug delivery, and biosensor systems. Chemical communications 2007:3236-45.
[7] Nasongkla N, Bey E, Ren J, Ai H, Khemtong C, Guthi JS, et al. Multifunctional Polymeric Micelles as Cancer-Targeted, MRI-Ultrasensitive Drug Delivery Systems. Nano Letters 2006;6:2427-30.
[8] Soppimath KS, Tan DCW, Yang YY. pH-Triggered Thermally Responsive Polymer Core–Shell Nanoparticles for Drug Delivery. Advanced materials 2005;17:318-23.
[9] Dromi S, Frenkel V, Luk A, Traughber B, Angstadt M, Bur M, et al. Pulsed-High Intensity Focused Ultrasound and Low Temperature–Sensitive Liposomes for Enhanced Targeted Drug Delivery and Antitumor Effect. Clinical Cancer Research 2007;13:2722-7.
[10] Yang H, Kao WJ. Synthesis and characterization of nanoscale dendritic RGD clusters for potential applications in tissue engineering and drug delivery. Int J Nanomedicine 2007;2:89-99.
[11] Maria V-R, Eduardo R-H, Blanca G, Alejandro B. Design of Smart Nanomaterials for Drug and Gene Delivery. Acc Chem Res 2011;1:6-29.
[12] Ambrogio MW, Thomas CR, Zhao Y-L, Zink JI, Stoddart JF. Mechanized Silica Nanoparticles: A New Frontier in Theranostic Nanomedicine. ACCOUNTS OF CHEMICAL RESEARCH 2011;44:903-13.
[13] An F-F, Cao W, Liang X-J. Nanostructural Systems Developed with Positive Charge Generation to Drug Delivery. Advanced Healthcare Materials 2014;3:1162-81.
[14] Yang KN, Zhang CQ, Wang W, Wang PC, Zhou JP, Liang XJ. pH-responsive mesoporous silica nanoparticles employed in controlled drug delivery systems for cancer treatment. Cancer Biol Med 2014;11:34-43.
[15] Vallet-Regí M, Balas F, Arcos D. Mesoporous Materials for Drug Delivery. Angewandte Chemie International Edition 2007;46:7548-58.
[16] Manzano M, Colilla M, Vallet-Regí M. Drug delivery from ordered mesoporous matrices. Expert Opinion on Drug Delivery 2009;6:1383-400.
[17] Yang P, Gai S, Lin J. Functionalized mesoporous silica materials for controlled drug delivery.

Chemical Society reviews 2012;41:3679-98.
[18] Manzano M, Vallet-Regi M. New developments in ordered mesoporous materials for drug delivery. Journal of Materials Chemistry 2010;20:5593-604.
[19] Mai WX, Meng H. Mesoporous silica nanoparticles: A multifunctional nano therapeutic system. Integrative biology : quantitative biosciences from nano to macro 2013;5:19-28.
[20] Soni G, Yadav KS. Nanogels as potential nanomedicine carrier for treatment of cancer: A mini review of the state of the art. Saudi Pharmaceutical Journal.
[21] Yallapu MM, Jaggi M, Chauhan SC. Design and engineering of nanogels for cancer treatment. Drug Discovery Today 2011;16:457-63.
[22] Jhaveri AM, Torchilin VP. Multifunctional polymeric micelles for delivery of drugs and siRNA. Frontiers in Pharmacology 2014;5:77.
[23] Maya SS, B., Nair A, Rejinold NS, Nair SV, Jayakumar R. Smart Stimuli Sensitive Nanogels in Cancer Drug Delivery and Imaging: A Review. Current Pharmaceutical Design 2013;19:15.
[24] Salas G, Costo R, Morales MdP. Synthesis of Inorganic Nanoparticles. Frontiers of Nanoscience 2012;4:35-65.
[25] Wagstaff AJ, Brown SD, Holden MR, Craig GE, Plumb JA, Brown RE, et al. Cisplatin drug delivery using gold-coated iron oxide nanoparticles for enhanced tumour targeting with external magnetic fields. Inorganica Chimica Acta 2012;393:328-33.
[26] Upadhyay D, Scalia S, Vogel R, Wheate N, Salama R, Young P, et al. Magnetised Thermo Responsive Lipid Vehicles for Targeted and Controlled Lung Drug Delivery. Pharm Res 2012;29:2456-67.
[27] Tapan K J, Morales MA, Sahoo SK, Leslie-Pelecky SL, Labhasetwar V. Iron Oxide Nanoparticles for Sustained Delivery of ANricancer Agents. Molecular pharmaceutics 2005;2:194-205.
[28] Perni S, Piccirillo C, Pratten J, Prokopovich P, Chrzanowski W, Parkin IP, et al. The antimicrobial properties of light-activated polymers containing methylene blue and gold nanoparticles. Biomaterials 2009;30:89-93.
[29] Dunnill CW, Kafizas A, Aiken ZA, Pratten J, Wilson M, Morgan DJ, et al. White Light Induced Photocatalytic Activity of Sulfur-Doped TiO2 Thin Films and their Potential for Antibacterial Application. Journal of Materials Chemistry 2009;in press.
[30] Douroumis D, Onyesom I, Maniruzzaman M, Mitchell J. Mesoporous silica nanoparticles in nanotechnology. Critical reviews in biotechnology 2012.
[31] Zhao Y, Vivero-Escoto JL, Slowing II, Trewyn BG, Lin VS-Y. Capped mesoporous silica nanoparticles as stimuli-responsive controlled release systems for intracellular drug/gene delivery. Expert Opinion on Drug Delivery 2010;7:1013-29.
[32] Rosenholm JM, Sahlgren C, Linden M. Towards multifunctional, targeted drug delivery systems using mesoporous silica nanoparticles--opportunities & challenges. Nanoscale 2010;2:1870-83.
[33] Vivero-Escoto JL, Slowing, II, Trewyn BG, Lin VS. Mesoporous silica nanoparticles for intracellular controlled drug delivery. Small 2010;6:1952-67.

[34] Lu J, Liong M, Zink JI, Tamanoi F. Mesoporous silica nanoparticles as a delivery system for hydrophobic anticancer drugs. Small 2007;3:1341-6.
[35] Colilla M, González B, Vallet-Regí M. Mesoporous silica nanoparticles for the design of smart delivery nanodevices. Biomaterials Science 2013;1:114.
[36] Lu J, Li Z, Zink JI, Tamanoi F. In vivo tumor suppression efficacy of mesoporous silica nanoparticles-based drug-delivery system: enhanced efficacy by folate modification. Nanomedicine : nanotechnology, biology, and medicine 2012;8:212-20.
[37] Gao Y, Chen Y, Ji X, He X, Yin Q, Zhang Z, et al. Controlled Intracellular Release of Doxorubicin in Multidrug-Resistant Cancer Cells by Tuning the Shell-Pore Sizes of Mesoporous Silica. AM CHEM SOC 2011;5:9788-98.
[38] Pérez-Quintanilla D, Gómez-Ruiz S, Žižak Ž, Sierra I, Prashar S, del Hierro I, et al. A New Generation of Anticancer Drugs: Mesoporous Materials Modified with Titanocene Complexes. Chemistry – A European Journal 2009;15:5588-97.
[39] Ahn B, Park J, Singha K, Park H, Kim WJ. Mesoporous silica nanoparticle-based cisplatin prodrug delivery and anticancer effect under reductive cellular environment. Journal of Materials Chemistry B 2013;1:2829-36.
[40] Lu J, Liong M, Zink JI, Tamanoi F. Mesoporous Silica Nanoparticles as a Delivery System for Hydrophobic Anticancer Drugs. Small 2007;3:1341-6.
[41] Chen C, Geng J, Pu F, Yang X, Ren J, Qu X. Polyvalent Nucleic Acid/Mesoporous Silica Nanoparticle Conjugates: Dual Stimuli-Responsive Vehicles for Intracellular Drug Delivery. Angewandte Chemie International Edition 2011;50:882-6.
[42] Zheng B, Xu S, Lin L, Wang Z, Feng Z, Zheng Z. Plasmon enhanced near-infrared quantum cutting of KYF 4: Tb 3+, Yb 3+ doped with Ag nanoparticles. Optics Letters 2015;40:2630-3.
[43] Férey G, Mellot-Draznieks C, Serre C, Millange F, Dutour J, Surblé S, et al. A Chromium Terephthalate-Based Solid with Unusually Large Pore Volumes and Surface Area. Science 2005;309:2040-2.
[44] Fan J, Yu C, Gao F, Lei J, Tian B, Wang L, et al. Cubic Mesoporous Silica with Large Controllable Entrance Sizes and Advanced Adsorption Properties. Angewandte Chemie International Edition 2003;42:3146-50.
[45] Azaïs T, Tourné-Péteilh C, Aussenac F, Baccile N, Coelho C, Devoisselle J-M, et al. Solid-State NMR Study of Ibuprofen Confined in MCM-41 Material. Chemistry of Materials 2006;18:6382-90.
[46] Yanes RE, Tamanoi F. Development of mesoporous silica nanomaterials as a vehicle for anticancer drug delivery. Ther Deliv 2012;3:389-404.
[47] Chen Y, Chen H, Zeng D, Tian Y, Chen F, Feng J, et al. Core/Shell Structured Hollow Mesoporous Nanocapsules: A Potential Platform for Simultaneous Cell Imaging and Anticancer Drug Delivery. ACS Nano 2010;4:6001-13.
[48] Lee JE, Lee N, Kim T, Kim J, Hyeon T. Multifunctional Mesoporous Silica Nanocomposite Nanoparticles for Teranostic Applications. ACCOUNTS OF CHEMICAL RESEARCH 2011;44:893-902.

[49] Kim J, Moon H, Kim T, Yang S, Park J, Naskar D, et al. Developing animal models for alveolar bone scaffolds and tissue engineering. JOURNAL OF TISSUE ENGINEERING AND REGENERATIVE MEDICINE: WILEY-BLACKWELL 111 RIVER ST, HOBOKEN 07030-5774, NJ USA; 2014. p. 495-6.
[50] Yang Q, Wang S, Fan P, Wang L, Di Y, Lin K, et al. pH-Responsive Carrier System Based on Carboxylic Acid Modified Mesoporous Silica and Polyelectrolyte for Drug Delivery. Chem Mater 2005;17:5999-6003.
[51] Xie M, Shi H, Ma K, Shen H, Li B, Shen S, et al. Hybrid nanoparticles for drug delivery and bioimaging: mesoporous silica nanoparticles functionalized with carboxyl groups and a near-infrared fluorescent dye. Journal of colloid and interface science 2013;395:306-14.
[52] Fan J, Fang G, Wang X, Zeng F, Xiang Y, Wu S. Targeted anticancer prodrug with mesoporous silica nanoparticles as vehicles. Nanotechnology 2011;22:455102.
[53] Lee C-H, Cheng S-H, Huang IP, Souris JS, Yang C-S, Mou C-Y, et al. Intracellular pH-Responsive Mesoporous Silica Nanoparticles for the Controlled Release of Anticancer Chemotherapeutics. Angewandte Chemie International Edition 2010;49:8214-9.
[54] Lin C-H, Cheng S-H, Liao W-N, Wei P-R, Sung P-J, Weng C-F, et al. Mesoporous silica nanoparticles for the improved anticancer efficacy of cis-platin. International journal of pharmaceutics 2012;429:138-47.
[55] Liu R, Zhang Y, Zhao X, Agarwal A, Mueller LJ, Feng P. pH-Responsive Nanogated Ensemble Based on Gold-Capped Mesoporous Silica through an Acid-Labile Acetal Linker. Journal of the American Chemical Society 2010;132:1500-1.
[56] Aznar E, Coll C, Marcos MD, Martínez-Máñez R, Sancenón F, Soto J, et al. Borate-Driven Gatelike Scaffolding Using Mesoporous Materials Functionalised with Saccharides. Chemistry – A European Journal 2009;15:6877-88.
[57] Gan Q, Lu X, Yuan Y, Qian J, Zhou H, Lu X, et al. A magnetic, reversible pH-responsive nanogated ensemble based on Fe3O4 nanoparticles-capped mesoporous silica. Biomaterials 2011;32:1932-42.
[58] Chen L, Di J, Cao C, Zhao Y, Ma Y, Luo J, et al. A pH-driven DNA nanoswitch for responsive controlled release. Chemical communications 2011;47:2850-2.
[59] Park C, Oh K, Lee SC, Kim C. Controlled Release of Guest Molecules from Mesoporous Silica Particles Based on a pH-Responsive Polypseudorotaxane Motif. Angewandte Chemie International Edition 2007;46:1455-7.
[60] Coti KK, Belowich ME, Liong M, Ambrogio MW, Lau YA, Khatib HA, et al. Mechanised nanoparticles for drug delivery. Nanoscale 2009;1:16-39.
[61] Saha S, Leung KCF, Nguyen TD, Stoddart JF, Zink JI. Nanovalves. Adv Funct Mater 2007;17:685-93.
[62] Zhao Y-L, Li Z, Kabehie S, Botros YY, Stoddart JF, Zink JI. pH-Operated Nanopistons on the Surfaces of Mesoporous Silica Nanoparticles. Journal of the American Chemical Society 2010;132:13016-25.

[63] Meng H, Xue M, Xia T, Zhao Y-L, Tamanoi F, Stoddart JF, et al. Autonomous in Vitro Anticancer Drug Release from Mesoporous Silica Nanoparticles by pH-Sensitive Nanovalves. Journal of the American Chemical Society 2010;132:12690-7.
[64] Muhammad F, Guo M, Qi W, Sun F, Wang A, Guo Y, et al. pH-Triggered Controlled Drug Release from Mesoporous Silica Nanoparticles via Intracelluar Dissolution of ZnO Nanolids. Journal of the American Chemical Society 2011;133:8778-81.
[65] Gao C, Zheng H, Xing L, Shu M, Che S. Designable Coordination Bonding in Mesopores as a pH-Responsive Release System. Chemistry of Materials 2010;22:5437-44.
[66] Popat A, Liu J, Lu GQ, Qiao SZ. A pH-responsive drug delivery system based on chitosan coated mesoporous silica nanoparticles. Journal of Materials Chemistry 2012;22:11173-8.
[67] Chen F, Zhu Y. Chitosan enclosed mesoporous silica nanoparticles as drug nano-carriers: Sensitive response to the narrow pH range. Microporous and Mesoporous Materials 2012;150:83-9.
[68] Tang H, Guo J, Sun Y, Chang B, Ren Q, Yang W. Facile synthesis of pH sensitive polymer-coated mesoporous silica nanoparticles and their application in drug delivery. International journal of pharmaceutics 2011;421:388-96.
[69] Murakami K, Yu X, Watanabe S, Kato T, Inoue Y, Sugawara K. Synthesis of thermosensitive polymer/mesoporous silica composite and its temperature dependence of anion exchange property. Journal of colloid and interface science 2011;354:771-6.
[70] Zintchenko A, Ogris M, Wagner E. Temperature Dependent Gene Expression Induced by PNIPAM-Based Copolymers: Potential of Hyperthermia in Gene Transfer. Bioconjugate Chemistry 2006;17:766-72.
[71] Nagase K, Kobayashi J, Kikuchi A, Akiyama Y, Kanazawa H, Okano T. Interfacial Property Modulation of Thermoresponsive Polymer Brush Surfaces and Their Interaction with Biomolecules. Langmuir : the ACS journal of surfaces and colloids 2007;23:9409-15.
[72] Keerl M, Smirnovas V, Winter R, Richtering W. Copolymer Microgels from Mono- and Disubstituted Acrylamides: Phase Behavior and Hydrogen Bonds. Macromolecules 2008;41:6830-6.
[73] Hoare T, Santamaria J, Goya GF, Irusta S, Lin D, Lau S, et al. A Magnetically Triggered Composite Membrane for On-Demand Drug Delivery. Nano letters 2009;9:3651-7.
[74] Schlossbauer A, Warncke S, Gramlich PME, Kecht J, Manetto A, Carell T, et al. A Programmable DNA-Based Molecular Valve for Colloidal Mesoporous Silica. Angewandte Chemie International Edition 2010;49:4734-7.
[75] Baeza A, Guisasola E, Ruiz-Hernández E, Vallet-Regí M. Magnetically Triggered Multidrug Release by Hybrid Mesoporous Silica Nanoparticles. Chemistry of Materials 2012;24:517-24.
[76] Lai C-Y, Trewyn BG, Jeftinija DM, Jeftinija K, Xu S, Jeftinija S, et al. A Mesoporous Silica Nanosphere-Based Carrier System with Chemically Removable CdS Nanoparticle Caps for Stimuli-Responsive Controlled Release of Neurotransmitters and Drug Molecules. Journal of the American Chemical Society 2003;125:4451-9.
[77] Giri S, Trewyn BG, Stellmaker MP, Lin VSY. Stimuli-Responsive Controlled-Release Delivery

System Based on Mesoporous Silica Nanorods Capped with Magnetic Nanoparticles. Angewandte Chemie International Edition 2005;44:5038-44.
[78] Torney F, Trewyn BG, Lin VSY, Wang K. Mesoporous silica nanoparticles deliver DNA and chemicals into plants. Nat Nano 2007;2:295-300.
[79] Nadrah P, Maver U, Jemec A, Tisler T, Bele M, Drazic G, et al. Hindered Disulfide Bonds to Regulate Release Rate of Model Drug from Mesoporous Silica. ACS applied materials & interfaces 2013.
[80] Liu R, Zhao X, Wu T, Feng P. Tunable Redox-Responsive Hybrid Nanogated Ensembles. Journal of the American Chemical Society 2008;130:14418-9.
[81] Luo Z, Cai K, Hu Y, Zhao L, Liu P, Duan L, et al. Mesoporous Silica Nanoparticles End-Capped with Collagen: Redox-Responsive Nanoreservoirs for Targeted Drug Delivery. Angewandte Chemie International Edition 2011;50:640-3.
[82] Climent E, Bernardos A, Martinez-Manez R, Maquieira A, Marcos MD, Pastor-Navarro N, et al. Controlled Delivery System Using Antibody-Capped Mesoporous Nanocontainers. Journal of the American Chemical Society 2009;131.
[83] Schlossbauer A, Kecht J, Bein T. Biotin–Avidin as a Protease-Responsive Cap System for Controlled Guest Release from Colloidal Mesoporous Silica. Angewandte Chemie International Edition 2009;48:3092-5.
[84] Bernardos A, Aznar E, Marcos MD, Martínez-Máñez R, Sancenón F, Soto J, et al. Enzyme-Responsive Controlled Release Using Mesoporous Silica Supports Capped with Lactose. Angewandte Chemie International Edition 2009;48:5884-7.
[85] Agostini A, Mondragón L, Coll C, Aznar E, Marcos MD, Martinez-Manez R, et al. ChemistryOpen 2012;1:17-20.
[86] Zhao Y, Trewyn BG, Slowing II, Lin VSY. Mesoporous Silica Nanoparticle-Based Double Drug Delivery System for Glucose-Responsive Controlled Release of Insulin and Cyclic AMP. Journal of the American Chemical Society 2009;131:8398-400.
[87] Ellington AD, Szostak JW. In vitro selection of RNA molecules that bind specific ligands. Nature 1990;346:818-22.
[88] Ozalp VC, Eyidogan F, Oktem HA. Aptamer-Gated Nanoparticles for Smart Drug Delivery. Pharmaceuticals 2011;4:1137-57.
[89] Zhu C-L, Lu C-H, Song X-Y, Yang H-H, Wang X-R. Bioresponsive Controlled Release Using Mesoporous Silica Nanoparticles Capped with Aptamer-Based Molecular Gate. Journal of the American Chemical Society 2011;133:1278-81.
[90] Özalp VC, Schäfer T. Aptamer-Based Switchable Nanovalves for Stimuli-Responsive Drug Delivery. Chemistry – A European Journal 2011;17:9893-6.
[91] Liu Y, Ding X, Li J, Luo Z, Hu Y, Liu J, et al. Enzyme responsive drug delivery system based on mesoporous silica nanoparticles for tumor therapy in vivo. Nanotechnology 2015;26:145102.
[92] Ferris DP, Zhao Y-L, Khashab NM, Khatib HA, Stoddart JF, Zink JI. Light-Operated Mechanized

Nanoparticles. Journal of the American Chemical Society 2009;131:1686-8.
[93] Wang Y, Li B, Zhang L, Song H, Zhang L. Targeted Delivery System Based on Magnetic Mesoporous Silica Nanocomposites with Light-Controlled Release Character. ACS applied materials & interfaces 2012;5:11-5.
[94] Yuan Q, Zhang Y, Chen T, Lu D, Zhao Z, Zhang X, et al. Photon-Manipulated Drug Release from a Mesoporous Nanocontainer Controlled by Azobenzene-Modified Nucleic Acid. ACS Nano 2012;6:6337-44.
[95] Park C, Lee K, Kim C. Photoresponsive Cyclodextrin-Covered Nanocontainers and Their Sol-Gel Transition Induced by Molecular Recognition. Angewandte Chemie International Edition 2009;48:1275-8.
[96] Mal NK, Fujiwara M, Tanaka Y. Photocontrolled reversible release of guest molecules from coumarin-modified mesoporous silica. Nature 2003;421:350-3.
[97] Knezevic NZ, Trewyn BG, Lin VSY. Functionalized mesoporous silica nanoparticle-based visible light responsive controlled release delivery system. Chemical Communications 2011;47:2817-9.
[98] Vivero-Escoto JL, Slowing II, Wu C-W, Lin VSY. Photoinduced Intracellular Controlled Release Drug Delivery in Human Cells by Gold-Capped Mesoporous Silica Nanosphere. Journal of the American Chemical Society 2009;131:3462-3.
[99] Lin Q, Huang Q, Li C, Bao C, Liu Z, Li F, et al. Anticancer Drug Release from a Mesoporous Silica Based Nanophotocage Regulated by Either a One- or Two-Photon Process. Journal of the American Chemical Society 2010;132:10645-7.
[100] Schwarz A, Stander S, Berneburg M, Bohm M, Kulms D, van Steeg H, et al. Interleukin-12 suppresses ultraviolet radiation-induced apoptosis by inducing DNA repair. Nat Cell Biol 2002;4:26-31.
[101] Juzenas P, Juzeniene A, Kaalhus O, Iani V, Moan J. Noninvasive fluorescence excitation spectroscopy during application of 5-aminolevulinic acid in vivo. Photochemical & Photobiological Sciences 2002;1:745-8.
[102] Liu H, Chen D, Li L, Liu T, Tan L, Wu X, et al. Multifunctional Gold Nanoshells on Silica Nanorattles: A Platform for the Combination of Photothermal Therapy and Chemotherapy with Low Systemic Toxicity. Angewandte Chemie International Edition 2011;50:891-5.
[103] Tang H, Shen S, Guo J, Chang B, Jiang X, Yang W. Gold nanorods@mSiO2 with a smart polymer shell responsive to heat/near-infrared light for chemo-photothermal therapy. Journal of Materials Chemistry 2012;22:16095-103.
[104] Fang W, Yang J, Gong J, Zheng N. Photo-and pH-triggered release of anticancer drugs from mesoporous silica-coated Pd@Ag nanoparticles. Adv Funct Mater 2012;22:842-8.
[105] Zhang Q, Iwakuma N, Sharma P, Moudgil BM, Wu C, McNeill J, et al. Gold nanoparticles as a contrast agent for in vivo tumor imaging with photoacoustic tomography. Nanotechnology 2009;20:395102.
[106] XIA Y, LI W, COBLEY CM, CHEN J, XIA X, ZHANG Q, et al. Gold Nanocages: From Synthesis to

Theranostic Applications. ACCOUNTS OF CHEMICAL RESEARCH 2011;44:914-24.
[107] Tran CTH, Kondyurin A, Chrzanowski W, Bilek MMM, McKenzie DR. Influence of pH on yeast immobilization on polystyrene surfaces modified by energetic ion bombardment. Colloids and Surfaces B: Biointerfaces 2013;104:145-52.
[108] You J, Zhang R, Xiong C, Zhong M, Melancon M, Gupta S, et al. Effective photothermal chemotherapy using doxorubicin-loaded gold nanospheres that target EphB4 receptors in tumors. Cancer research 2012;72:4777-86.
[109] Tan MC, Ying JY, Chow GM. Interfacial properties and in vitro cytotoxic effects of surface-modified near infrared absorbing Au-Au(2)S nanoparticles. Journal of materials science Materials in medicine 2009;20:2091-103.
[110] Leung KC, Xuan S, Zhu X, Wang D, Chak CP, Lee SF, et al. Gold and iron oxide hybrid nanocomposite materials. Chem Soc Rev 2012;41:1911-28.
[111] Shen S, Tang H, Zhang X, Ren J, Pang Z, Wang D, et al. Targeting mesoporous silica-encapsulated gold nanorods for chemo-photothermal therapy with near-infrared radiation. Biomaterials 2013;34:3150-8.
[112] Singh NS, Kulkarni H, Pradhan L, Bahadur D. A multifunctional biphasic suspension of mesoporous silica encapsulated with YVO4:Eu3+ and Fe3O4 nanoparticles: synergistic effect towards cancer therapy and imaging Nanotechnology 2013;24:065101.
[113] Chen J, Glaus C, Laforest R, Zhang Q, Yang M, Gidding M, et al. Gold nanocages as photothermal transducers for cancer treatment. Small 2010;6:811-7.
[114] Fedoryshin LL, Tavares AJ, Petryayeva E, Doughan S, Krull UJ. Near-Infrared-Triggered Anticancer Drug Release from Upconverting Nanoparticles. ACS applied materials & interfaces 2014;6:13600-6.
[115] Pei W-B, Chen B, Wang L, Wu J, Teng X, Lau R, et al. NaF-mediated controlled-synthesis of multicolor Na x ScF 3+ x: Yb/Er upconversion nanocrystals. Nanoscale 2015;7:4048-54.
[116] Liu J, Bu W, Pan L, Shi J. NIR-Triggered Anticancer Drug Delivery by Upconverting Nanoparticles with Integrated Azobenzene-Modified Mesoporous Silica. Angewandte Chemie International Edition 2013;52:4375-9.
[117] Ruggiero E, Hernández-Gil J, Mareque-Rivas JC, Salassa L. Near infrared activation of an anticancer Pt IV complex by Tm-doped upconversion nanoparticles. Chemical Communications 2015.
[118] Chen Q, Wang C, Cheng L, He W, Cheng Z, Liu Z. Protein modified upconversion nanoparticles for imaging-guided combined photothermal and photodynamic therapy. Biomaterials 2014;35:2915-23.
[119] Wang C, Cheng L, Liu Z. Upconversion nanoparticles for photodynamic therapy and other cancer therapeutics. Theranostics 2013;3:317.
[120] Zhang X, Tian G, Yin W, Wang L, Zheng X, Yan L, et al. Controllable Generation of Nitric Oxide by Near-Infrared-Sensitized Upconversion Nanoparticles for Tumor Therapy. Advanced

Functional Materials 2015;25:3049-56.
[121] Liu J, Wang C, Wang X, Wang X, Cheng L, Li Y, et al. Mesoporous Silica Coated Single-Walled Carbon Nanotubes as a Multifunctional Light-Responsive Platform for Cancer Combination Therapy. Advanced Functional Materials 2015;25:384-92.
[122] Fan W, Shen B, Bu W, Chen F, He Q, Zhao K, et al. A smart upconversion-based mesoporous silica nanotheranostic system for synergetic chemo-/radio-/photodynamic therapy and simultaneous MR/UCL imaging. Biomaterials 2014;35:8992-9002.
[123] Guo H, Qian H, Idris NM, Zhang Y. Singlet oxygen-induced apoptosis of cancer cells using upconversion fluorescent nanoparticles as a carrier of photosensitizer. Nanomedicine: Nanotechnology, Biology and Medicine 2010;6:486-95.
[124] Dühnen S, Rinkel T, Haase M. Size control of nearly monodisperse β-NaGdF4 particles prepared from small α-NaGdF4 nanocrystals. Chemistry of Materials 2015.
[125] Cheng L, Wang C, Liu Z. Upconversion nanoparticles and their composite nanostructures for biomedical imaging and cancer therapy. Nanoscale 2013;5:23-37.
[126] Chen Y, Ai K, Liu J, Sun G, Yin Q, Lu L. Multifunctional envelope-type mesoporous silica nanoparticles for pH-responsive drug delivery and magnetic resonance imaging. Biomaterials 2015;60:111-20.
[127] Lu S, Tu D, Hu P, Xu J, Li R, Wang M, et al. Multifunctional Nano-Bioprobes Based on Rattle-Structured Upconverting Luminescent Nanoparticles. Angewandte Chemie International Edition 2015.
[128] Yang Y, Sun Y, Cao T, Peng J, Liu Y, Wu Y, et al. Hydrothermal synthesis of NaLuF 4: 153 Sm, Yb, Tm nanoparticles and their application in dual-modality upconversion luminescence and SPECT bioimaging. Biomaterials 2013;34:774-83.
[129] Xia A, Chen M, Gao Y, Wu D, Feng W, Li F. Gd 3+ complex-modified NaLuF 4-based upconversion nanophosphors for trimodality imaging of NIR-to-NIR upconversion luminescence, X-Ray computed tomography and magnetic resonance. Biomaterials 2012;33:5394-405.
[130] Schäfer H, Ptacek P, Zerzouf O, Haase M. Synthesis and optical properties of KYF4/Yb, Er nanocrystals, and their surface modification with undoped KYF4. Advanced Functional Materials 2008;18:2913-8.
[131] Tian G, Zheng X, Zhang X, Yin W, Yu J, Wang D, et al. TPGS-stabilized NaYbF 4: Er upconversion nanoparticles for dual-modal fluorescent/CT imaging and anticancer drug delivery to overcome multi-drug resistance. Biomaterials 2015;40:107-16.
[132] Ju Q, Chen X, Ai F, Peng D, Lin X, Kong W, et al. An upconversion nanoprobe operating in the first biological window. Journal of Materials Chemistry B 2015;3:3548-55.
[133] Gayathri S, Ghosh OSN, Sudhakara P, Viswanath AK. Chitosan conjugation: A facile approach to enhance the cell viability of LaF 3: Yb, Er upconverting nanotransducers in human breast cancer cells. Carbohydrate Polymers 2015;121:302-8.
[134] Chen G, Shen J, Ohulchanskyy TY, Patel NJ, Kutikov A, Li Z, et al. (α-NaYbF4: Tm3+)/CaF2

core/shell nanoparticles with efficient near-infrared to near-infrared upconversion for high-contrast deep tissue bioimaging. ACS nano 2012;6:8280-7.
[135] Dong N-N, Pedroni M, Piccinelli F, Conti G, Sbarbati A, Ramírez-Hernández JE, et al. NIR-to-NIR two-photon excited CaF2: Tm3+, Yb3+ nanoparticles: multifunctional nanoprobes for highly penetrating fluorescence bio-imaging. ACS nano 2011;5:8665-71.
[136] Zhang C, Li C, Peng C, Chai R, Huang S, Yang D, et al. Facile and controllable synthesis of monodisperse CaF2 and CaF2: Ce3+/Tb3+ hollow spheres as efficient luminescent materials and smart drug carriers. Chemistry-A European Journal 2010;16:5672-80.
[137] Wang J, Wang F, Wang C, Liu Z, Liu X. Single-Band Upconversion Emission in Lanthanide-Doped KMnF3 Nanocrystals. Angewandte Chemie International Edition 2011;50:10369-72.
[138] Gayathri S, Ghosh OSN, Viswanath AK, Sudhakara P, Reddy MJK, Shanmugharaj A. Synthesis of YF 3: Yb, Er upconverting nanofluorophores using chitosan and their cytotoxicity in MCF-7 cells. International journal of biological macromolecules 2015;72:1308-12.
[139] Qiu X, Lin T. Multicolor Emission Tuning and Red/Green Ratio Enhancement of Yb 3/Er 3 Co-Doped KGdF4 Upconversion Nanoparticles. Journal of Nanomaterials 2015;501:361957.
[140] Wang C, Tao H, Cheng L, Liu Z. Near-infrared light induced in vivo photodynamic therapy of cancer based on upconversion nanoparticles. Biomaterials 2011;32:6145-54.
[141] Qiao X-F, Zhou J-C, Xiao J-W, Wang Y-F, Sun L-D, Yan C-H. Triple-functional core–shell structured upconversion luminescent nanoparticles covalently grafted with photosensitizer for luminescent, magnetic resonance imaging and photodynamic therapy in vitro. Nanoscale 2012;4:4611-23.
[142] Li X, Zhou L, Wei Y, El-Toni AM, Zhang F, Zhao D. Anisotropic Growth-Induced Synthesis of Dual-Compartment Janus Mesoporous Silica Nanoparticles for Bimodal Triggered Drugs Delivery. Journal of the American Chemical Society 2014;136:15086-92.
[143] Zhou J, Liu Z, Li F. Upconversion nanophosphors for small-animal imaging. Chemical Society Reviews 2012;41:1323-49.
[144] Tian G, Gu Z, Zhou L, Yin W, Liu X, Yan L, et al. Mn2+ Dopant-Controlled Synthesis of NaYF4: Yb/Er Upconversion Nanoparticles for in vivo Imaging and Drug Delivery. Advanced Materials 2012;24:1226-31.
[145] Wang M, Abbineni G, Clevenger A, Mao C, Xu S. Upconversion nanoparticles: synthesis, surface modification and biological applications. Nanomedicine: Nanotechnology, Biology and Medicine 2011;7:710-29.
[146] Kim JE, Shin JY, Cho MH. Magnetic nanoparticles: an update of application for drug delivery and possible toxic effects. Archives of toxicology 2012;86:685-700.
[147] Wahajuddin, Arora S. Superparamagnetic iron oxide nanoparticles: magnetic nanoplatforms as drug carriers. International journal of nanomedicine 2012;7:3445-71.
[148] Maeng JH, Lee DH, Jung KH, Bae YH, Park IS, Jeong S, et al. Multifunctional doxorubicin

loaded superparamagnetic iron oxide nanoparticles for chemotherapy and magnetic resonance imaging in liver cancer. Biomaterials 2010;31:4995-5006.

[149] Chen P-J, Hu S-H, Hsiao C-S, Chen Y-Y, Liu D-M, Chen S-Y. Multifunctional magnetically removable nanogated lids of Fe3O4-capped mesoporous silica nanoparticles for intracellular controlled release and MR imaging. Journal of Materials Chemistry 2011;21:2535-43.

[150] Lee JE, Lee N, Kim H, Kim J, Choi SH, Kim JH, et al. Uniform Mesoporous Dye-Doped Silica Nanoparticles Decorated with Multiple Magnetite Nanocrystals for Simultaneous Enhanced Magnetic Resonance Imaging, Fluorescence Imaging, and Drug Delivery. Journal of the American Chemical Society 2009;132:552-7.

[151] Thomas CR, Ferris DP, Lee J-H, Choi E, Cho MH, Kim ES, et al. Noninvasive Remote-Controlled Release of Drug Molecules in Vitro Using Magnetic Actuation of Mechanized Nanoparticles. Journal of the American Chemical Society 2010;132:10623-5.

[152] Bringas E, Koysuren O, Quach DV, Mahmoudi M, Aznar E, Roehling JD, et al. Triggered release in lipid bilayer-capped mesoporous silica nanoparticles containing SPION using an alternating magnetic field. Chemical Communications 2012;48:5647-9.

[153] Ruiz-Hernández E, Baeza A, Vallet-Regí M. Smart Drug Delivery through DNA/Magnetic Nanoparticle Gates. ACS Nano 2011;5:1259-66.

[154] Chang B, Sha X, Guo J, Jiao Y, Wang C, Yang W. Thermo and pH dual responsive, polymer shell coated, magnetic mesoporous silica nanoparticles for controlled drug release. Journal of Materials Chemistry 2011;21:9239-47.

[155] Casasús R, Climent E, Marcos MD, Martínez-Máñez R, Sancenón F, Soto J, et al. Dual Aperture Control on pH- and Anion-Driven Supramolecular Nanoscopic Hybrid Gate-like Ensembles. Journal of the American Chemical Society 2008;130:1903-17.

[156] Angelos S, Yang Y-W, Khashab NM, Stoddart JF, Zink JI. Dual-Controlled Nanoparticles Exhibiting AND Logic. Journal of the American Chemical Society 2009;131:11344-6.

[157] Wu S, Huang X, Du X. Glucose- and pH-Responsive Controlled Release of Cargo from Protein-Gated Carbohydrate-Functionalized Mesoporous Silica Nanocontainers. Angewandte Chemie International Edition 2013;52:5580-4.